to explain the VCD. For amino vibrations, current can be generated both in the ligand ring and in the ring closed by a bridging halide ion. The VCD spectra of these metal complexes appear to be completely dominated by ring-current effects, which mask any coupled oscillator VCD contributions.

Further examples of ring-current-enhanced VCD in transition-metal complexes have been observed for β-alanine ligands, which form six-membered rings,[39] and α-amino acid ligands, which form five-membered chelate rings.[40] These results, which will be reported separately, confirm and extend the mechanisms proposed here for the CH and NH stretching VCD of ethylenediamine ligands.

Acknowledgment. We acknowledge financial support from grants from the National Science Foundation (CHE83-02416) and the National Institutes of Health (GM-23567). We are grateful to Faye Ratnowsky for carrying out some of the syntheses and resolutions of the cobalt complexes.

(39) Freedman, T. B.; Young, D. A.; Nafie, L. A., unpublished results.

(40) Freedman, T. B.; Young, D. A.; Oboodi, M. R.; Nafie, L. A., submitted for publication.

Aqueous Coordination Chemistry of Vanadocene Dichloride, $V(\eta^5\text{-}C_5H_5)_2Cl_2$, with Nucleotides and Phosphoesters. Mechanistic Implications for a New Class of Antitumor Agents

Jeffrey H. Toney,† Carolyn P. Brock, and Tobin J. Marks*

Contribution from the Department of Chemistry, Northwestern University, Evanston, Illinois 60201. *Received March 14, 1986*

Abstract: This paper reports an investigation of the mode of interaction of the organometallic antitumor agent Cp_2VCl_2 (Cp = η^5-C_5H_5) with nucleotides and phosphoesters, in aqueous solution near physiological pH, employing high-field ^1H and ^{31}P FT NMR and EPR. Paramagnetic (d^1) aqueous Cp_2VCl_2 is found to selectively interact with the phosphate functionalities of nucleotides and to significantly shorten the ^{31}P nuclear relaxation times. A quantitative analysis of the paramagnetic contributions to the longitudinal (T_1) and transverse (T_2) relaxation rates of the ^{31}P nucleus of 2′-deoxyadenosine-5′-monophosphate reveals that the average internuclear vanadium–phosphorus distance in the solution complex is 6.2 (2) or 5.5 (1) Å, depending on whether each vanadium ion interacts with one or two phosphate moieties, respectively. The temperature dependence of the ^{31}P relaxation rates yields kinetic parameters characterizing the labile outer-sphere complexation of aqueous Cp_2VCl_2 to the phosphate groups. At 25 °C, the mean lifetime of the metal–nucleotide complex is estimated to be 0.49 (8) ms. Activation parameters for the ligand dissociation at 25 °C are the following: $\Delta G^\ddagger$ = 19.5 (2.6) kcal/mol, $\Delta H^\ddagger$ = 13.8 (1.0) kcal/mol, and $\Delta S^\ddagger$ = −19.1 (4.3) e.u. Nucleotide–nucleotide Watson–Crick base-pairing is not disrupted by Cp_2VCl_2 in aqueous solution, as shown by ^1H NMR. An X-ray crystallographic study was also carried out on the model compound, $Cp_2V(OH_2)_2{\cdot}2O_2P(OPh)_2$ (**1**). The crystal structure of **1** serves to define the coordination of the Cp_2V^{2+} unit to a diesterified phosphoric acid, which possesses metrical parameters similar to those of polynucleotides. The complex crystallizes in the monoclinic space group $P2_1$ (No. 4) with four molecules in a unit cell of dimensions a = 10.571 (2) Å, b = 12.108 (3) Å, c = 25.277 (6) Å, and β = 98.50 (2)° at 163 (2) K. Least-squares refinement led to a value for the conventional R index (on F) of 0.031 for 6197 unique reflections having $2\theta_{MoK\alpha} \leq 55°$ and $I > 3\sigma(I)$. The molecular structure consists of pseudotetrahedral $V(\eta^5\text{-}C_5H_5)_2(OH_2)_2^{2+}$ cations connected to diphenyl phosphate anions via strong hydrogen bonds. Average metrical parameters for the $V(\eta^5\text{-}C_5H_5)_2(OH_2)_2^{2+}$ cation are as follows: V–C distance, 2.297 (5) Å; V–O(water) distance, 2.050 (8) Å; ring centroid–V–ring centroid angle, 133.0 (4)°. Average metrical parameters for the $PO_2(OPh)_2^-$ anion are P–OPh distance, 1.601 (6) Å; P–O (non-ester), 1.480 (2) Å; and C–O distance, 1.392 (3) Å, and these are typical for a phosphodiester anion. The vanadium–phosphorus nonbonded contacts are in the range 5.07–6.44 Å, in good agreement with the nucleotide NMR results in solution. Implications of these results for the observed biological activity of Cp_2VCl_2 are briefly discussed.

Köpf and Köpf-Maier have shown that metallocene dihalides and bis(pseudohalides) of the constitution Cp_2MX_2 (A) where Cp = η^5-C_5H_5, M = Ti, V, Nb, Mo[1-6]; X = F, Cl, Br, I, NCS, and N_3,[7] are highly active agents against Ehrlich ascites tumor (EAT) cells, lymphoid leukemia L1210, lymphocytic leukemia P388,[8] and most recently, human colon carcinoma heterotransplanted to athymic mice.[9] In addition, we have recently shown that Cp_2VCl_2 is highly active against human epidermoid (HEP-2) tumor cells in vitro as well as intraperitoneal (ip) implants of a

A

† Present address: Laboratory of Biochemical Pharmacology, Dana-Farber Cancer Institute, Harvard Medical School, Boston, MA 02115.

(1) Köpf, H.; Köpf-Maier, P. *Angew. Chem., Int. Ed. Engl.* **1979**, *18*, 477–478.
(2) Köpf-Maier, P.; Hesse, B.; Köpf, H. *J. Cancer Res. Clin. Oncol.* **1980**, *96*, 43–51.
(3) Köpf-Maier, P.; Köpf, H. *Z. Naturforsch. B.: Anorg. Chem., Org. Chem.* **1979**, *34b*, 805–807.
(4) Köpf-Maier, P.; Leitner, M.; Köpf, H. *J. Inorg. Nucl. Chem.* **1980**, *42*, 1789–1791.
(5) Köpf-Maier, P.; Leitner, M.; Voigtländer, R.; Köpf, H. *Z. Naturforsch. B.: Anorg. Chem., Org. Chem.* **1979**, *34c*, 1174–1176.
(6) Köpf-Maier, P.; Hesse, B.; Voigtländer, R.; Köpf, H. *J. Cancer Res. Clin. Oncol.* **1980**, *97*, 31–39.
(7) Köpf-Maier, P.; Wagner, W.; Hesse, B.; Köpf, H. *Eur. J. Cancer* **1981**, *17* (6), 665–669.
(8) Köpf-Maier, P.; Wagner, W.; Köpf, H. *Cancer Chemother. Pharmacol.* **1981**, *5*, 237–241.

0002-7863/86/1508-7263$01.50/0 © 1986 American Chemical Society

Chart I

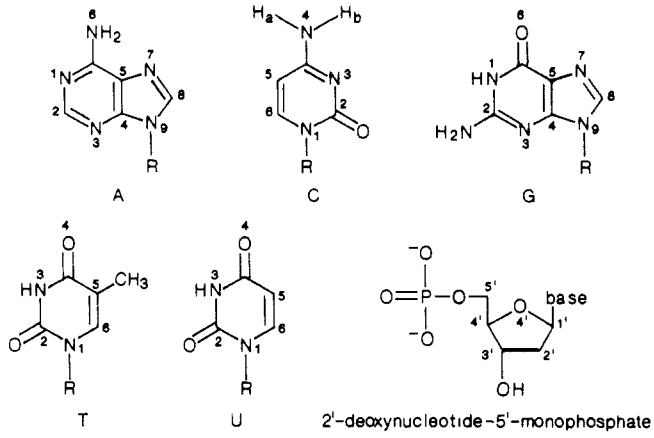

mouse mammary tumor (TA3Ha) in vivo.[10] The Cp_2MX_2 compounds thus constitute a potent new class of organometallic antitumor agents.

Analogies between the metallocene dihalides and the well-known antitumor agent *cis*-dichlorodiammineplatinum(II) ("cisplatin") and derivatives thereof[11,12] have been drawn since both classes of compounds possess metrically similar *cis*-MX_2 functionalities. That the carcinostatic activity of Cp_2MX_2 agents may be mechanistically similar to cisplatin is also suggested by observations of inhibition of nucleic acid metabolism[13,14] and mitotic activity[15] as well as by evidence for the accumulation of the respective metals in the nuclear heterochromatin of the tumor cells.[15-17] The primary biological target for both classes of compounds is thus proposed to be DNA.[12,15] Since the primary structure of DNA is comprised of arrays of 2'-deoxyribonucleotide-5'-monophosphates, it would clearly be of interest to investigate the nature of the binding between a representative metallocene dihalide and nucleotides or phosphate esters under conditions approximating physiological/therapeutic (mM in Cp_2MX_2, pH near neutrality).

An accurate description of the nature of Cp_2MX_2–biomolecule interactions depends first on a detailed knowledge of the aqueous chemistry of the Cp_2MX_2 complexes. We have recently described in detail the hydrolysis chemistry of the Cp_2MX_2 compounds where M = Ti, V, and Zr and X = Cl.[18] The chloride aquation in all of these compounds was shown to be more rapid and more extensive than that in cisplatin. However, only Cp_2VCl_2 was found to possess an M–(η^5-C_5H_5) bond with significant long-term hydrolytic stability at physiological pH. It is for this chemical reason as well as for its magnetic properties that Cp_2VCl_2 is attractive for studying Cp_2MX_2–biomolecule interactions. The paramagnetism of vanadium(IV) (d^1) and long electron spin–lattice relaxation time (10^{-8}–10^{-9} s)[19] renders this complex an ideal NMR solution structural (relaxation) probe. If a labile complex is formed between such a paramagnetic probe and a diamagnetic ligand, ligand nuclei proximate to the site(s) of interaction will be preferentially relaxed in well-understood ways.[20,21] It is thereby possible to obtain both kinetic and structural information on the binding.

We present here a chemical/physicochemical investigation of interactions between aqueous Cp_2VCl_2 and DNA constituents, including the 2'-deoxynucleotide-5'-monophosphates (dNMPs; N = adenosine (A), cytidine (C), guanosine (G), thymidine (T), and uridine (U)—see Chart I), alkylated nucleobases (see Chart I) as well as related mono- and phosphodiesters in aqueous solution, employing high-field FT NMR. The concentration ranges employed for the nucleotides and phosphate esters were chosen to conform to those used previously for NMR studies of these compounds.[22,23] It will be seen that Cp_2VCl_2 exhibits high selectivity for binding to phosphate groups of the nucleotides relative to sites on purine or pyrimidine bases. A detailed study of the effect of Cp_2VCl_2 on the ^{31}P longitudinal and transverse relaxation rates of a representative nucleotide allows an estimation of the average V^{IV}–^{31}P distance as well as kinetic parameters for the Cp_2V^{2+}–phosphate interaction. The interaction of aqueous vanadocene dichloride with DNA constituents will be seen to be radically different from that of cisplatin with regard to both the structural and kinetic aspects of binding. We also report here an X-ray crystal-structure analysis of the model compound $Cp_2V(OH_2)_2{\cdot}2O_2P(OPh)_2$ (**1**) which details the geometry and nature of Cp_2V^{2+}–phosphate binding to a DNA-related[24] phosphodiester and is relevant to the aforementioned solution spectroscopic studies.

Experimental Section

Methods and Materials. All organometallic compounds were handled under prepurified nitrogen with use of standard Schlenk techniques. Organic solvents were thoroughly dried and deoxygenated in a manner appropriate to each. Water was doubly distilled, deionized (resistance ~17 M Ω^{-1} cm^{-1}), and thoroughly saturated with prepurified nitrogen. The complex Cp_2VCl_2 (Strem Chemical Co., Newburyport, MA) was purified by anaerobic Soxhlet extraction with CH_2Cl_2 (under partial vacuum). The purity was checked by IR and EPR spectroscopy. Me_2SO-d_6 (Aldrich Chemical Co., 99.9 atom % D) was dried by transferring onto freshly activated molecular sieves (4 Å) and then stirring with powdered BaO overnight. All other chemicals were reagent grade. Deoxynucleotide monophosphates (disodium salts) and alkylated nucleobases were obtained from Sigma Chemical Co. and used as received. Purity was verified by ^1H and ^{31}P NMR.

Physical Measurements. ^1H NMR spectra were recorded on a JEOL FX-270 FT instrument (16K data points) with use of solvent suppression techniques[25,26] for spectra taken in H_2O. In this case, a co-axial D_2O insert was used for locking. All spectra were recorded with 6.3° flip angles (pulse width = 1.4 μs). Reported chemical shifts are referenced to internal H_2O (4.63 ppm). Integration studies employed appropriate pulse delays (5.0 s); relative peak areas were established by cutting and weighing. Measurement of cyclopentadiene loss from Cp_2VCl_2 during the experiments was carried out as described previously.[18] Infrared spectra were recorded on Perkin-Elmer 599 or 283 spectrometers. Sample mulls were prepared in a glovebox with dry, degassed Nujol and were

(9) Köpf-Maier, P.; Moormann, A.; Köpf, H. *Eur. J. Cancer Clin. Oncol.* **1985**, *21*, 853–857.
(10) (a) Toney, J. H.; Rao, L. N.; Murthy, M. S.; Marks, T. J. *Breast Cancer Res. Treat.* **1985**, *6*, 185. (b) Toney, J. H.; Rao, L. N.; Murthy, M. S.; Marks, T. J., submitted for publication. (c) Murthy, M. S.; Toney, J. H.; Rao, L. N.; Kuo, L. Y.; Marks, T. J. *Proc. Am. Assoc. Cancer Res.* **1986**, *27*, 279.
(11) For authoritative reviews of cisplatin chemistry and biology, see: (a) "Platinum, Gold, and Other Metal Chemotherapeutic Agents", Lippard, S. J., Ed. *ACS Symp. Ser.* **1983**, *209*. (b) Marcelis, A. T. M.; Reedijk, J. *Recueil* **1983**, *102* (3), 121–129.
(12) For authoritative reviews of the proposed mechanisms of action of platinum antitumor compounds, see: (a) Roberts, J. J.; Thomson, A. J. *Prog. Nucl. Acid Res. Mol. Biol.* **1979**, *22*, 71–133. (b) Prestayko, A. W.; Crooke, S. T.; Carter, S. K., Eds. *Cisplatin Current Status and New Developments*; Academic Press, Inc.: New York, 1980. (c) Hacker, M. P.; Douple, E. B.; Krakoff, I. H., Eds. *Platinum Coordination Complexes in Chemotherapy*; Nijhoff Publishers: Boston, MA, 1984. (d) Rosenberg, B. *Cancer* **1985**, *55*, 2303–2316.
(13) Köpf-Maier, P.; Köpf, H. *Naturwissenschaften* **1980**, *67*, 415–416.
(14) Köpf-Maier, P.; Wagner, W.; Köpf, H. *Naturwissenschaften* **1981**, *68*, 272–273.
(15) Köpf, H.; Köpf-Maier, P., ref 11a, Chapter 16, pp 315–333.
(16) Köpf-Maier, P.; Köpf, H. *Naturwissenschaften* **1981**, *68*, 273–274.
(17) Köpf-Maier, P.; Krahl, D. *Chem.-Biol. Interact.* **1983**, *44*, 317–328.
(18) Toney, J. H.; Marks, T. J. *J. Am. Chem. Soc.* **1985**, *107*, 947–953.
(19) (a) James, T. L. *Nuclear Magnetic Resonance in Biochemistry*; Academic Press: New York, 1975; p 179. (b) Reuben, J.; Fiat, D. *J. Am. Chem. Soc.* **1969**, *91*, 4652–4656. (c) Wüthrich, K.; Connick, R. E. *Inorg. Chem.* **1968**, *7*, 1377–1388 and references therein.
(20) (a) Campbell, I. D.; Dwek, R. A. *Biological Spectroscopy*; The Benjamin/Cummings Publishing Co., Inc.: Menlo Park, CA, 1984; pp 127–177. (b) Jardetzky, O.; Roberts, G. C. K. *NMR in Molecular Biology*; Academic Press: New York, 1981; pp 83–114. (c) Reference 19a, Chapter 8. (d) Dwek, R. A. *Nuclear Magnetic Resonance in Biochemistry*; Oxford University Press (Clarendon): London, 1973; Chapters 9 and 10. (e) Carrington, A.; McLachlan, A. D. *Introduction to Magnetic Resonance*; Harper & Row: New York, 1967; Chapter 13.
(21) Natusch, D. F. S. *J. Am. Chem. Soc.* **1973**, *95*, 1688–1690.
(22) (a) Granot, J.; Feigon, J.; Kearns, D. R. *Biopolymers* **1982**, *21*, 181–201. (b) Granot, J.; Kearns, D. R. *Biopolymers* **1982**, *21*, 203–218.
(23) Raszka, M.; Kaplan, N. O. *Proc. Natl. Acad. Sci. U.S.A.* **1972**, *69*, 2025–2029.
(24) Saenger, W. *Principles of Nucleic Acid Structure*; Springer-Verlag: New York, 1984; pp 253–282.
(25) Hore, P. J. *J. Magn. Reson.* **1983**, *54*, 539–542.
(26) Hore, P. J. *J. Magn. Reson.* **1983**, *55*, 283–300.

studied between KBr plates in an air-tight, O-ring sealed holder. Calibration was accomplished with polystyrene.

^{31}P NMR spectra were recorded on a JEOL FX-270 FT instrument operating at 109.16 MHz (16K data points). The acquisition time was 0.409 s. All spectra were recorded with 79.7° flip angles (pulse width = 15.5 μs). Reported chemical shifts are relative to external 85% H_3PO_4 in H_2O. Spectra measured in H_2O (3.0 mL volume in a 10 mm Wilmad sample tube) employed a 4 mm co-axial D_2O insert for deuterium locking. ^1H broadbrand decoupling was applied during the measurements. Reported shifts are not corrected for bulk susceptibility effects, which are expected to be less than ca. 0.1 ppm at these Cp_2VCl_2 concentrations. Longitudinal relaxation times (T_1) were determined with use of a standard 180°–τ–90° pulse sequence, and transverse relaxation times (T_2) were determined with use of the observed line width of the resonance ($\Delta\nu_{1/2} = (\pi T_2)^{-1}$ assuming a Lorentzian line shape and negligible instrumental broadening). In the T_2 measurements, a sweep width of 2000 Hz was used (0.244 Hz per data point) for greater accuracy. ^{31}P NMR spectra measured at 36.19 MHz were recorded on a JEOL FX-90 FT instrument, and spectra at 161.903 MHz were recorded on a Varian XL400 GS FT instrument.

EPR spectra were recorded on a Varian E-4 spectrometer (using a Varian TE 102 cavity), and g values were calibrated with a Varian strong pitch (0.1% in KCl) standard (g value 2.0028). EPR samples in H_2O or Me_2SO were studied in 1.0-mm capillaries (outer diameter) to minimize dielectric loss.[27]

Measurements of pH were performed with a Beckman SS-2 "Expandomatic" pH meter and a Broadley-Jones pH electrode having an internal reference (4 M KCl saturated with AgCl).

Isolation and Characterization of $Cp_2V(OH_2)_2{\cdot}2O_2P(OPh)_2$ (1). A weighed quantity of Cp_2VCl_2 (77 mg, 0.31 mmol) was dissolved in doubly distilled deionized water under nitrogen (10 mL, 31 mM) at room temperature in a Schlenk tube. After being stirred for about 1 h, the solution was filtered through a Schlenk frit. Under N_2, the resulting filtrate was then carefully layered onto a previously filtered aqueous solution (10 mL, 63 mM) of diphenyl phosphate (saturated with N_2) (157 mg, 0.63 mmol), using a gas-tight syringe. After the solution was left to stand overnight, beautiful aquamarine crystals formed in the diphenyl phosphate layer (final pH 2.00). The aqueous solution was decanted by syringe, and the crystals were washed three times under N_2 with a minimal amount of ice-cold, doubly distilled deionized water and dried in vacuo to yield ~80 mg (~40% yield) of **1**. These crystals were found to be slightly air-sensitive, developing a brown coating after standing in air for more than 1–2 days. IR data (cm^{-1}): 3120 w, 1600 m, 1465 m, 1252 m, 1213 m, 1093 m, 1073 w, 1030 w, 907 m, 775 w, 748 w, 693 w, 613 vw, 545 w. ^1H NMR data (Me_2SO-d_6): multiplets at δ 7.44 and 7.22. ^{31}P NMR data (Me_2SO-d_6): +10.93 ppm. EPR data (Me_2SO-d_6): eight-line spectrum, $g_{iso} = 2.02$ (1), A_{iso} (^{51}V) = 73 ± 2 G. Anal. (Galbraith (V, P), Dornis and Kolbe (C, H, Cl)) Calcd for $V(Cp)_2(OH_2)_2{\cdot}2PO_2(OPh)_2$: C, 57.06, H, 4.76; V, 7.13; P, 8.67; Cl, 0.00. Found: C, 57.42; H, 5.09; V, 6.73; P, 9.15; Cl, 0.0.

X-ray Crystallographic Study of $Cp_2V(OH_2)_2{\cdot}2O_2P(OPh)_2$ (1).[28] The compound crystallizes as aquamarine tablets in the monoclinic system with a = 10.571 (2) Å, b = 12.108 (3) Å, c = 25.277 (6) Å, β = 98.50 (2)°, and Z = 4 at 163 (2) K. The extinctions ($0k0$, $k = 2n + 1$) correspond either to the space group $P2_1$ (No. 4) or to $P2_1/m$ (No. 11). The crystal morphology and the distribution of the reflection intensities point to the noncentrosymmetric group; this choice was confirmed by the subsequent structure solution and refinement. There are two full formula units in the asymmetric unit. All data with $h, k \geq 0$ and $2\theta \leq 55°$ were measured on an Enraf-Nonius CAD4 diffractometer with Mo Kα radiation and a graphite monochromator (7649 unique reflections; 395 measured more than once; R factor on I for averaging = 0.018). No correction was made for absorption (crystal size: 0.3 × 0.3 × 0.4 mm; μ = 4.56 cm^{-1}); there was no evidence of decomposition or extinction. The positions of the V and P atoms were determined with the direct methods package MITHRIL;[29] all but one of the C atoms were then located with DIRDIF.[30] Hydrogen atoms on the phenyl groups were included as fixed contributions [r(C–H) = 1.00 Å; $B = 1.3B_{eq}$ for the attached C atom]. The H atoms of the water ligands could not be located. Anomalous terms were included for all non-hydrogen atoms, but the chirality of the crystal studied could not be determined. The structure was refined (Enraf-Nonius structure determination package;[31] neutral atom scattering factors;[32] full-matrix least-squares) to agreement factors R and R_w on F_o of 0.031 and 0.040 for 846 variables and the 6197 observations having $F_o^2 > 3\sigma(F_o^2)$. The error in an observation of unit weight is 1.42. The final difference Fourier map is essentially featureless; the largest peak has height 0.24 e $Å^{-3}$.

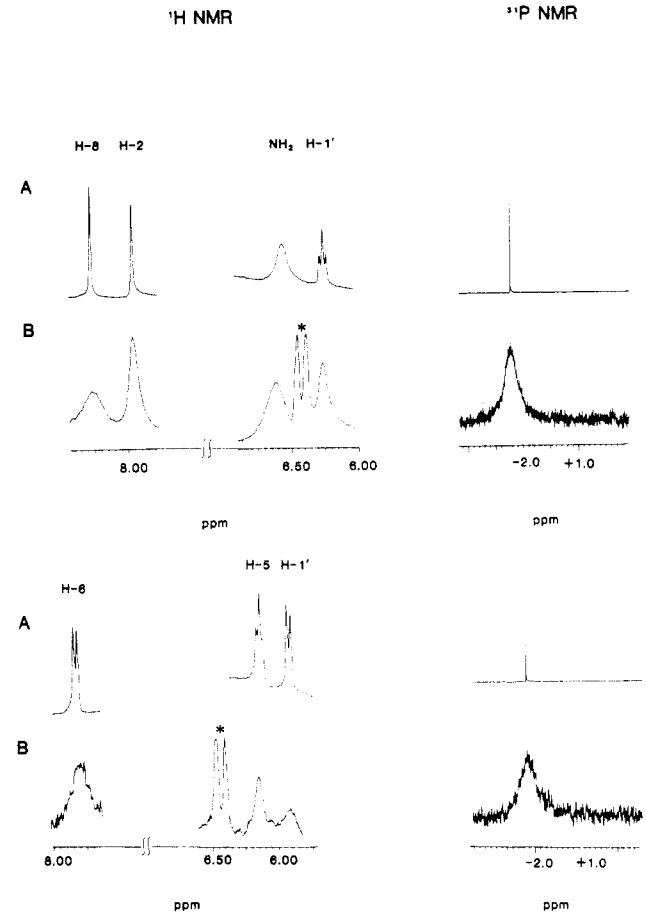

Figure 1. ^1H (270 MHz) and ^{31}P (109.16 MHz) NMR spectra of dAMP (51 mM) (top) and dCMP (42 mM) (bottom) in the presence of (A) 0.0 equiv of Cp_2VCl_2 or (B) 0.50 equiv of Cp_2VCl_2 in H_2O at room temperature. The asterisk indicates multiplets due to olefinic protons of free cyclopentadiene. Spectra were taken 2 h after mixing.

Results

The primary focus of this investigation was to obtain structural and kinetic information on the binding of aqueous Cp_2VCl_2 (V(IV), d^1) to DNA constituents and models thereof in aqueous solution by studying NMR relaxation effects caused by the paramagnetic V(IV) center. The interaction between aqueous Cp_2VCl_2 and the nucleotides was investigated first.

Interaction of Aqueous Cp_2VCl_2 with 2′-Deoxyribonucleotide-5′-monophosphates. The binding mode of aqueous Cp_2VCl_2 to nucleotides was investigated by ^1H (270 MHz) and ^{31}P (109 MHz) NMR in H_2O. The ^1H NMR assignments can be made according to well-documented spectral analyses.[23,33,34] At room temperature, only the carbon-bound protons of the nucleotides can be readily observed by ^1H NMR in H_2O (with the exception of the amino group on dAMP). Nitrogen-bound protons can only be observed at or below 0 °C in H_2O, since the rate of proton exchange with

(27) Hyde, J. S. *Rev. Sci. Instrum.* **1972**, *43*, 629–631 and references therein.
(28) See paragraph at end of paper regarding supplementary material.
(29) Gilmore, C. J. *J. Appl. Crystallogr.* **1984**, *17*, 42–46.
(30) Beurskens, P. T.; Bosman, W. P.; Doesburg, H. M.; Gould, R. O.; van den Hark, Th. E. M.; Prick, P. A.; Noordik, J. H.; Beurskens, G.; Parthasarthi, V.; Bruinsslot, H. J.; Haltiwanger, R. C. *DIRDIF*; Crystallography Laboratory, Toernooiveld, Technical Report 1983/1, 6525 ED Nikmegan, Netherlands, 1983.
(31) Enraf-Nonius Structure Determination Package. B. A. Frenz & Associates, College Station, Texas; and Enraf-Nonius, Delft, 1985.
(32) Cromer, D. T.; Waber, J. T. *International Tables for X-ray Crystallography*; Kynoch: Birmingham, 1974; Vol. IV, Tables 2.2B and 2.3.1. (Present distributor, D. Reidel, Dordrecht.)
(33) Davies, D. B. In *Progress in NMR Spectroscopy*; Emsley, J. W., Feeney, J., Sutcliffe, L. H., Eds.; Pergamon: Oxford, 1978; Vol. 12, Part 3, pp 135–225.
(34) Chottard, J.-C.; Girault, J.-P.; Guittet, E. R.; Lallemard, J.-Y.; Chottard, G., in ref 11a, Chapter 6, pp 125–145.

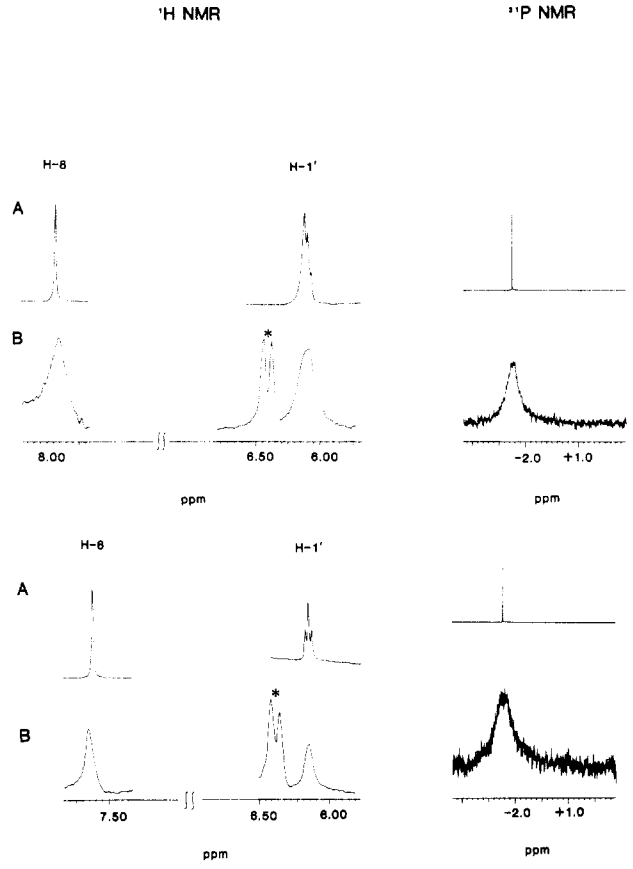

Figure 2. ^1H (270 MHz) and ^{31}P (109.16 MHz) NMR spectra of dGMP (48 mM) (top) and dTMP (41 mM) (bottom) in the presence of (A) 0.0 equiv of Cp_2VCl_2 or (B) 0.50 equiv of Cp_2VCl_2 in H_2O at room temperature. The asterisk indicates multiplets due to olefinic protons of free cyclopentadiene. Spectra were taken 2 h after mixing.

water is rapid on the NMR time scale at room temperature.[23] The nucleotides were also studied by ^{31}P NMR, employing samples identical with those used in the ^1H NMR experiments (same concentration in nucleotide and Cp_2VCl_2, pH, and temperature). Initial ^1H and ^{31}P NMR experiments involved the addition of 0.5 equiv of Cp_2VCl_2 to unbuffered solutions of the pure nucleotides (the pH values of the resulting solutions were typically ca. 6.5). Supplemental experiments were also carried out at exactly physiological pH. Thus, adjusting (with NaOH) a sample of deoxyadenosine monophosphate, in the presence of Cp_2VCl_2, to pH 7.4 did not significantly alter the ^1H and ^{31}P line widths from those observed at pH 6.5.

In the case of dAMP, addition of 0.5 equiv of Cp_2VCl_2 leads to modest broadening in the ^1H NMR (Figure 1) with no significant changes in the chemical shifts. A minor amount of free cyclopentadiene (C_5H_6), ca. 0.12 mol/mol of Cp_2VCl_2 (initial pH = 6.20), is observed after 2 h. Interestingly, the ^1H signal of adenosine position H(8) exhibits slight preferential broadening relative to H(2) (paramagnetic contributions to the line widths are 34 and 22 Hz for H(8) and H(2), respectively). This suggests that the V(IV) center may be in slightly greater time-averaged proximity to the N(7) site of the purine ring. No preferential broadening is observed in the resonances of the deoxyribose protons. In contrast, the ^{31}P signal of dAMP is greatly broadened by Cp_2VCl_2. The ^{31}P NMR line width increases from 3.0 Hz for the pure nucleotide to 285 Hz in the presence of 0.5 equiv of Cp_2VCl_2 (see Table I). The ^{31}P chemical shift is not significantly affected.

Figure 1 also shows that V(IV) induces only minor broadening of the ^1H signals of dCMP. Loss of ca. 0.17 mol of C_5H_6/mol of Cp_2VCl_2 is also observed (about 2 h after mixing; initial pH = 6.50). Slight preferential broadening of H(6) relative to H(5) and H(1′) is evident, suggesting that the V(IV) center may be in slightly greater time-averaged proximity to the deoxyribose ring.

Table I. ^{31}P NMR Spectral Characteristics of Nucleotides and Phenyl Phosphate in the Presence of 0.5 equiv of Cp_2VCl_2 (20–25 mM) in H_2O[a]

compound[b]	$\Delta\nu_{1/2p}$[c] (Hz)	ppm[d] no V(IV)	ppm[d] with V(IV)
dAMP	285	−2.48	−2.31
dCMP	321	−2.13	−2.11
dGMP	275	−2.56	−2.50
dTMP	419	−2.27	−2.30
dUMP	348	−1.96	−2.47
phenyl phosphate	459	+1.45	+0.94

[a] At 25 °C. [b] All compounds were added as disodium salts. [c] $\Delta\nu_{1/2p} = \Delta\nu_{1/2}$(with V(IV)) − $\Delta\nu_{1/2}$(without V(IV)). Average standard deviation = 7%. [d] Chemical shifts are relative to 85% H_3PO_4 in H_2O with D_2O insert for deuterium locking.

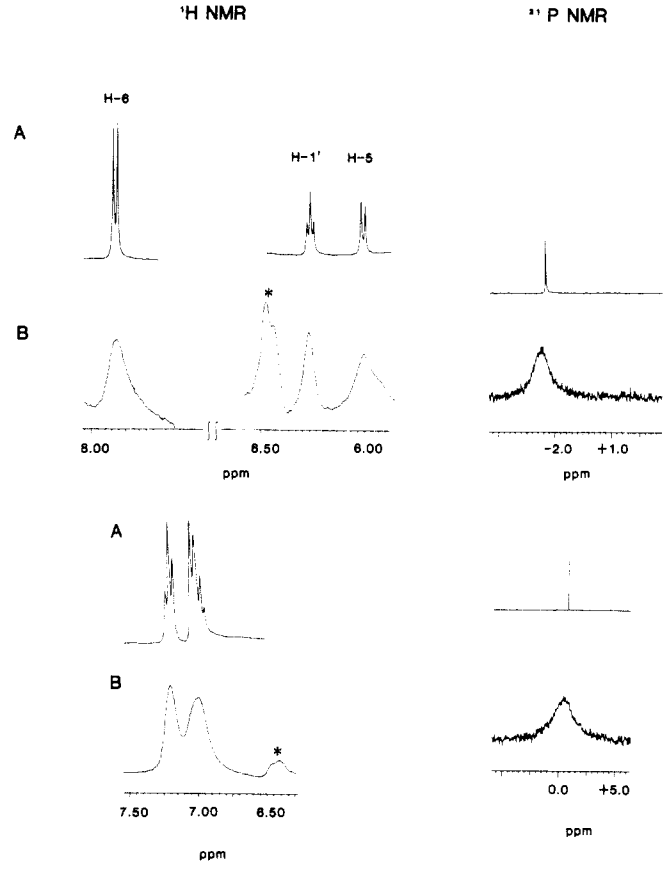

Figure 3. ^1H (270 MHz) and ^{31}P (109.16 MHz) NMR spectra of dUMP (47 mM) (top) and $PhOPO_3^{2-}$ (49 mM) (bottom) in the presence of (A) 0.0 equiv of Cp_2VCl_2 or (B) 0.50 equiv of Cp_2VCl_2 in H_2O at room temperature. The asterisk indicates multiplets due to olefinic protons of free cyclopentadiene. Spectra were taken 2 h after mixing.

Paramagnetic contributions to the line widths are ca. 33, 12, and 6 Hz for H(6), H(1′), and H(5), respectively. However, as observed for dAMP, the ^{31}P resonance is broadened greatly from 3.7 Hz for the pure nucleotide to 321 Hz in the presence of 0.5 equiv of Cp_2VCl_2, with no detectable change in the chemical shift.

In the case of dGMP, dTMP, and dUMP, V(IV) causes only minor broadening of the ^1H resonances, with no apparent selectivity (Figures 2 and 3). The paramagnetic contributions to the line widths for the H(1′) resonance are 23, 11, and 8 Hz for dGMP, dTMP, and dUMP, respectively. The H(5) resonance of dUMP is broadened somewhat more (paramagnetic contribution to the line width ≈25 Hz). Formation of C_5H_6 in these samples (about two hours after mixing) is estimated to be ca. 0.085, (initial pH = 6.48), 0.18 (initial pH = 6.48), and 0.24 (initial pH = 6.59) mol/mol of Cp_2VCl_2 for dGMP, dTMP, and dUMP, respectively. Upon addition of 0.5 equiv of Cp_2VCl_2, the ^{31}P resonance is significantly broadened (but not appreciably shifted), for all of these nucleotides, from 3.0 Hz for the pure

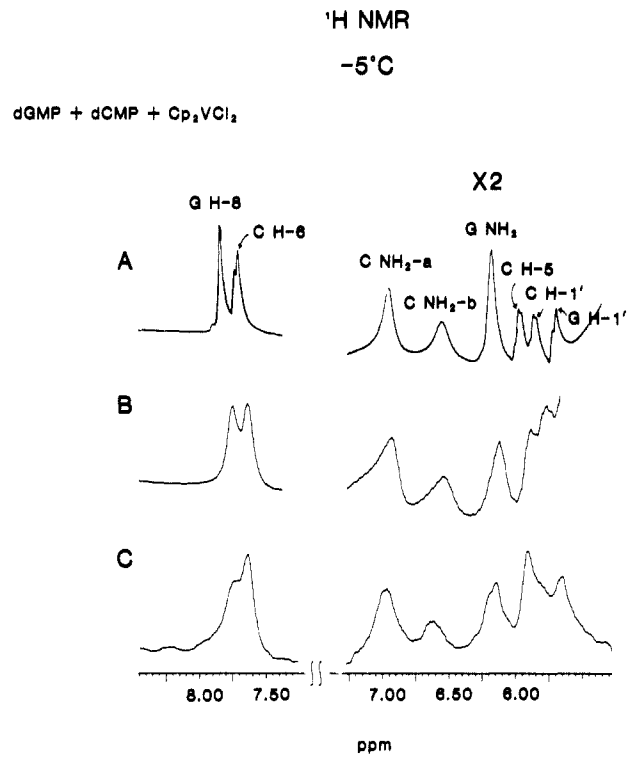

Figure 4. ^{1}H (270 MHz) NMR of dCMP and dGMP (0.20 M in each) in the presence of (A) 0.0 equiv of Cp_2VCl_2, (B) 0.06 equiv of Cp_2VCl_2, or (C) 0.32 equiv of Cp_2VCl_2 in H_2O at −5 °C. See Chart I for atom labeling. Spectra were taken 1 to 2 h after mixing.

nucleotides to 275, 419, and 348 Hz for dGMP, dTMP, and dUMP, respectively. Nearly identical behavior is observed with phenyl phosphate ($PhOPO_3^{2-}$) under identical conditions (Figure 3). The paramagnetic contribution to the line width for the aromatic resonance is only ca. 10 Hz (0.14 mol of C_5H_6/mol of Cp_2VCl_2 released within 2 h; initial pH = 6.05), while the ^{31}P NMR spectrum shows substantial broadening. The ^{31}P line width increases from 2.6 Hz for pure phenyl phosphate to 459 Hz in the presence of 0.5 equiv of Cp_2VCl_2 (no significant change in chemical shift). A similar experiment could not be carried out with diphenyl phosphate, since crystals of **1** form immediately (vide infra).

The effect of Cp_2VCl_2 on the Watson–Crick hydrogen bonding (base-pairing) between nucleotides in aqueous solution was also studied. Evidence for hydrogen bonding in aqueous solution is found in the ^{1}H NMR of GMP + CMP[23,35,36] and AMP + UMP.[23,37] Since the A–U base-pairing tendency is much weaker than that for G–C, the effect of Cp_2VCl_2 on the G–C interaction was investigated first. Spectra were recorded at −5 °C and pH 7.40 to decrease the rate of exchange between the amino protons and the solvent. Under these conditions of temperature and pH, the protons involved in hydrogen bonding can be readily observed. Addition of Cp_2VCl_2 to a mixture of dCMP and dGMP (1:1 molar ratio, 0.2 M in each) causes only minor broadening of the ^{1}H resonances and does not significantly affect the chemical shifts of the amino protons (for up to 0.32 equiv of Cp_2VCl_2—see Figure 4). Major changes in chemical shifts would be expected if the base-pairing were disrupted.[23,35–38] As observed with the individual mononucleotides, the ^{31}P resonances were significantly broadened by Cp_2VCl_2 (ca. 73 Hz for 0.32 equiv of Cp_2VCl_2). The effect of Cp_2VCl_2 on base-pairing between dAMP and dTMP (1:1 molar ratio) was studied in Me_2SO-d_6, since the hydrogen bonding is known to be stronger in this solvent than in water.[39] Addition of Cp_2VCl_2 to the dAMP–dTMP base pair in Me_2SO-d_6 causes only minor broadening of ^{1}H resonances, with no significant change in the chemical shifts (up to 0.40 equiv of Cp_2VCl_2) but significant broadening of the ^{31}P resonance (ca. 73 Hz for 0.4 equiv of Cp_2VCl_2) as observed with the dCMP–dGMP base pair in H_2O (vide supra).

Nuclear Relaxation Time Studies of a Selected Nucleotide (dAMP) in the Presence of Cp_2VCl_2. Vanadocene dichloride has been shown to exhibit high selectivity with regard to broadening of the ^{31}P resonance in all of the nucleotides relative to the proton nuclei. The broadening induced by Cp_2VCl_2 is qualitatively the same for the five nucleotides studied, as well as for phenyl phosphate. It was thus of interest to carry out a detailed quantitative study of the effect of this paramagnetic probe on the transverse and longitudinal relaxation rates of the phosphorus nucleus in a representative nucleotide, dAMP.

The paramagnetic contributions to the longitudinal (T_1) and transverse (T_2) relaxation times of a spin 1/2 nucleus (^{31}P) with gyromagnetic ratio γ bound near a paramagnetic site are given by the Solomon–Bloembergen equations:[20,40]

$$\frac{1}{T_{ip}} = \frac{f}{T_{iM} + \tau_M}, \quad i = 1 \text{ or } 2 \tag{1}$$

$$T_{1M}^{-1} = \frac{2}{15}\frac{S(S+1)\gamma^2 g^2 \beta^2}{r^6}\left(\frac{3\tau_c}{1+\omega_I^2\tau_c^2} + \frac{7\tau_c}{1+\omega_S^2\tau_c^2}\right) + \frac{2}{3}\frac{S(S+1)A^2}{\hbar^2}\left(\frac{\tau_e}{1+\omega_S^2\tau_e^2}\right) \tag{2}$$

$$T_{2M}^{-1} = \frac{1}{15}\frac{S(S+1)\gamma^2 g^2 \beta^2}{r^6}\left(4\tau_c + \frac{3\tau_c}{1+\omega_I^2\tau_c^2} + \frac{13\tau_c}{1+\omega_S^2\tau_c^2}\right) + \frac{1}{3}\frac{S(S+1)A^2}{\hbar^2}\left(\tau_e + \frac{\tau_e}{1+\omega_S^2\tau_e^2}\right) \tag{3}$$

In eq 1, T_{ip}^{-1} is the paramagnetic contribution to the longitudinal (i = 1) or transverse (i = 2) relaxation rate, f is the metal-to-nucleotide ratio, and τ_M is the mean lifetime of the metal–nucleotide complex. The intrinsic bound state relaxation rates, T_{iM}^{-1}, are given by eq 2 and 3, where S is the electron spin quantum number (S = 1/2 for V(IV)), g is the electronic g factor (g_{iso} = 1.985 for Cp_2V^{2+} systems),[41] β is the Bohr magneton, ω_I and ω_S are the Larmor angular precession frequencies ($\omega = 2\pi\nu$) for the nuclear and electron spin, respectively; and τ_c and τ_e are the correlation times for the dipolar (through space) and scalar (through bond) interactions, respectively. A is the electron–nuclear (^{51}V–^{31}P) superhyperfine coupling constant, and r is the average V(IV)–^{31}P distance of the ligand–metal complex in solution. Equations 4 and 5 relate τ_c and τ_e to the isotropic rotational correlation time (τ_R) and the longitudinal electron spin relaxation time (τ_{1s}).

$$\tau_c^{-1} = \tau_R^{-1} + \tau_e^{-1} \tag{4}$$

$$\tau_e^{-1} = \tau_M^{-1} + \tau_{1S}^{-1} \tag{5}$$

The parameters of greatest interest in describing Cp_2V^{2+}/nucleotide interactions are τ_M and r. To quantitatively analyze ^{31}P

(35) Walmsley, J. A.; Barr, R. G.; Bouhoutsos-Brown, E.; Pinnavaia, T. J. *J. Phys. Chem.* **1984**, *88*, 2599–2605.
(36) Sagan, B. L.; Walmsley, J. A. *Biochem. Biophys. Res. Commun.* **1985**, *128*, 980–986.
(37) Iwahashi, H.; Sugeta, H.; Kyogaku, Y. *Biochemistry* **1982**, *21*, 631–638.
(38) (a) Schöllhorn, H.; Raudaschl-Sieber, G.; Müller, G.; Thewalt, U.; Lippert, B. *J. Am. Chem. Soc.* **1985**, *107*, 5932–5937. (b) Beyerle, R.; Lippert, B. *Inorg. Chim. Acta* **1982**, *66*, 141–146. (c) Faggiani, R.; Lock, C. J. L.; Lippert, B. *J. Am. Chem. Soc.* **1980**, *102*, 5418–5419. (d) Lippert, B. *J. Am. Chem. Soc.* **1981**, *103*, 5691–5697. (e) Lippert, B. *Inorg. Chim. Acta* **1981**, *56*, L23–L24.
(39) Saenger, W. *Principles of Nucleic Acid Structure*; Springer-Verlag: New York, 1984; pp 126–131.
(40) Cunningham, B. A.; Raushel, F. M.; Villafranca, J. J.; Benkovic, S. J. *Biochemistry* **1981**, *20*, 359–362.
(41) (a) Petersen, J. L.; Dahl, L. F. *J. Am. Chem. Soc.* **1975**, *97*, 6416–6422. (b) Petersen, J. L.; Dahl, L. F. *J. Am. Chem. Soc.* **1975**, *97*, 6422–6433.
(42) (a) Reference 20b, pp 179–190. (b) Swift, T. J. In *NMR of Paramagnetic Molecules*; La Mar, G. N., Harrocks, W. DeW., Jr.; Holm, R. H., Eds.; Academic: New York, 1973; p 77.

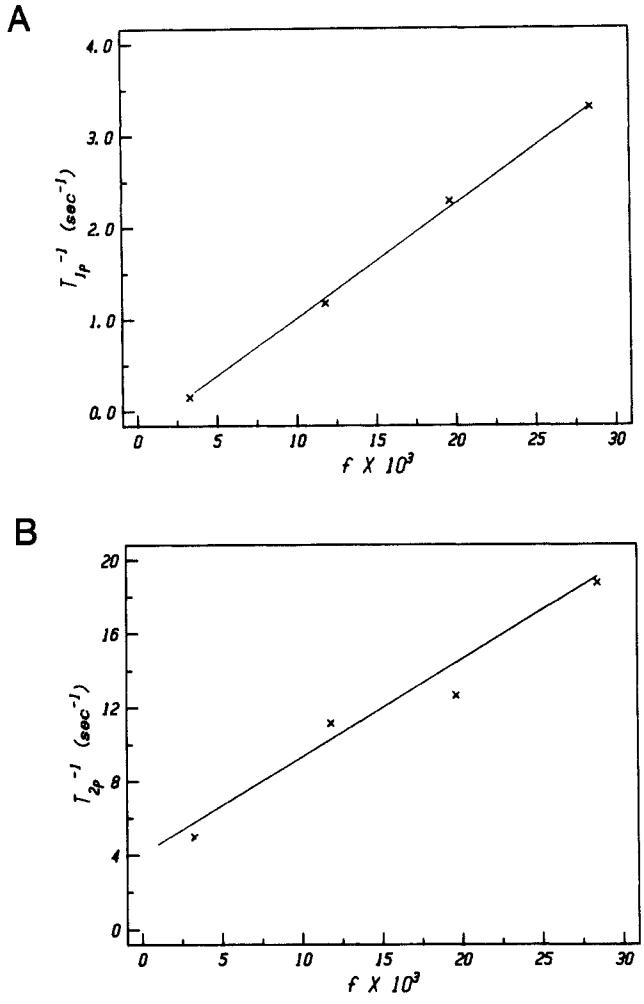

Figure 5. (A) T_{1p}^{-1} vs. f plot (f = $(Cp_2VCl_2)/(dAMP)$) for the ^{31}P nucleus (109.16 MHz) of dAMP (0.20 M) at room temperature. The line drawn through the data points indicates the linear least-squares fit. Correlation coefficient = 0.9993. (B) T_{2p}^{-1} vs. f plot for the ^{31}P nucleus (109.16 MHz) of dAMP (0.20 M) at room temperatures. The line drawn through the data points indicates the linear least-squares fit. Correlation coefficient = 0.9814.

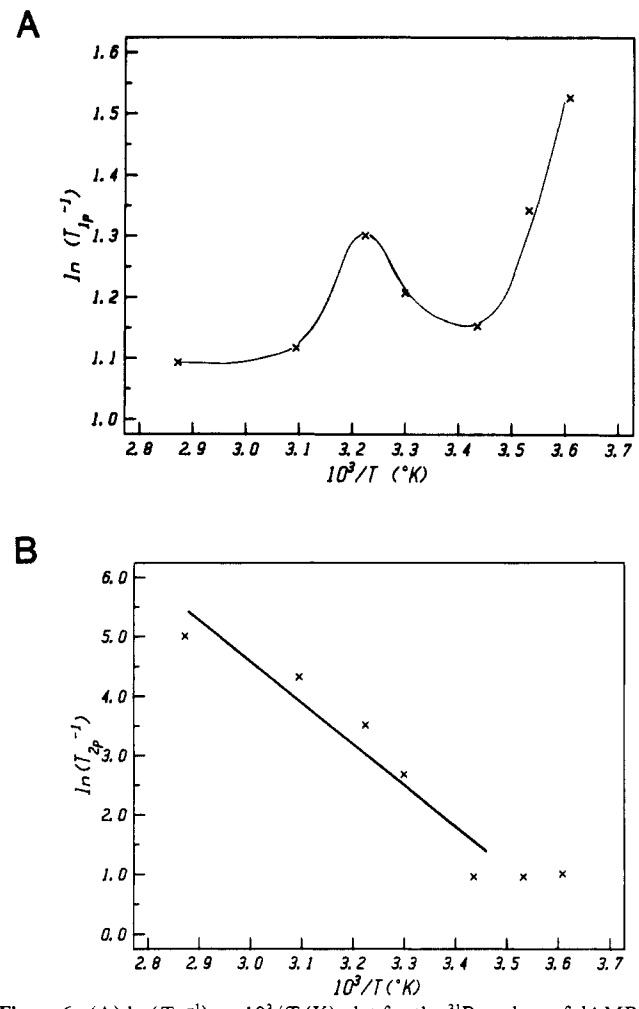

Figure 6. (A) ln (T_{1p}^{-1}) vs. $10^3/T$ (K) plot for the ^{31}P nucleus of dAMP (0.20 M) in the presence of 0.029 equiv of Cp_2VCl_2. The line through the data points is drawn as a guide to the eye. (B) ln (T_{2p}^{-1}) vs. $10^3/T$ (K) plot for the ^{31}P nucleus of dAMP (0.20 M) in the presence of 0.029 equiv of Cp_2VCl_2. The line drawn through the data points above the temperature where self-association becomes significant (ca. 10 °C) indicates the linear least-squares fit. Correlation coefficient = 0.9480 (five data points).

relaxation data via the Solomon–Bloembergen equations, it is necessary to make several pragmatic and reasonable assumptions.[20,22,42] First, it can be safely assumed[20,22] that $A(^{51}V) \ll \omega_S$. We find that the isotropic electron–^{51}V hyperfine coupling constant for aqueous Cp_2VCl_2 is typically (there is a slight pH dependence) ca. 75 G (2.1×10^8 Hz), so that $A(^{51}V) \sim 0.034\ \omega_S$. It is also assumed that the V(IV) g value is isotropic. Justification is found in single-crystal EPR studies of Cp_2VCl_2,[41] where g is nearly isotropic. The assumption that the V(IV) zero-field splitting is negligible (or at least $\ll\omega_S$) is, of course, expected for an $S = 1/2$ system. Since studies of VO_2^{2+} indicate that $\tau_{1S} \sim \tau_{2S}$,[19b,c] it is plausible to postulate that the present results are governed by a single electron relaxation time.[20,22] Lastly, we make the common,[20,22] physically reasonable assumptions that the relaxation arises from a single, isotropic motion and that correlation times for all types of motions are exponential. Since the electron spin relaxation time for V(IV) is relatively long (ca. 10^{-8}–10^{-9} s),[19] it is also reasonable to neglect the hyperfine (or scalar) term (vide infra) in eq 2. Equation 2 can thus be simplified to:[22]

$$r\ (\text{Å}) = C\left[T_{1M}\left(\frac{3\tau_c}{1 + \omega_I^2\tau_c^2}\right)\right]^{1/6} \qquad (6)$$

where $C = 398$ Å $s^{-1/3}$ for the V(IV)–^{31}P interaction.

When the above simplified relationship (eq 6) is used, the distance between the paramagnetic center, V(IV), and the ^{31}P nucleus in the dAMP ligand can be calculated, if a labile complex is formed in solution (vide infra). To accomplish this analysis, ^{31}P longitudinal and transverse relaxation rates of dAMP (0.16–0.20 M) were measured at 109.16 MHz for varying concentrations of Cp_2VCl_2 (0–4.5 mM). Data are summarized in Figure 5, A and B. The observed linearity in the f (f = $Cp_2VCl_2/dAMP$) vs. T_{1p}^{-1} and T_{2p}^{-1} plots suggests relatively strong binding of the V(IV) center to the dAMP ligand. The ratio of T_{1p}/T_{2p} obtained from the slopes of plots A and B in Figure 5 is estimated to be about 4.2 at 25 °C.

The temperature dependence of the net paramagnetic contributions to the relaxation rates was also studied. Data are summarized in Figure 6, A and B. The maximum observed for T_{1p}^{-1} (occurring at $10^3/T = 3.2$ or about 37 °C, see Figure 6A) argues that the longitudinal paramagnetic relaxation is dominated by a single correlation time,[22,43,44] and that $\tau_c = (\omega_I)^{-1} \approx 1.5$ (5) ns. The increase in line width of the ^{31}P resonance with increasing temperature (Figure 6B) is indicative of slow (becoming fast) chemical exchange.[22] The data points measured below 10 °C show anomalous behavior, since the resonances do not continue to sharpen as the temperature is lowered. This could be attributed to self-association of the nucleotide in solution and/or attainment of the slow exchange limit.[45]

(43) Niccolai, N.; Tiezzi, E.; Valeusin, G. *Chem. Rev.* **1982**, *82*, 359–384.
(44) Reference 19a, p 186.
(45) Karpel, R. L.; Kustin, K.; Wolff, M. A. *Isr. J. Chem.* **1973**, *11*, 735–748.

Activation parameters can be obtained for the V(IV)–^{31}P interaction by fitting the temperature dependence of the transverse relaxation rate to the relationship:[22,46]

$$\tau_M^{-1} = \frac{kT}{\hbar}\left(\frac{\Delta H^\ddagger}{RT} + \frac{\Delta S^\ddagger}{R}\right) \quad (7)$$

Since the temperature dependence of T_{2p}^{-1} is indicative of slow chemical exchange, τ_M can be estimated by $\tau_M = 1/fT_{2p}$ ($\tau_M \gg T_{2M}$). By fitting the τ_M vs. $1/T$ data to eq 7 with least-squares techniques (omitting data points below 10 °C), the following activation parameters are calculated at 25 °C: $\Delta G^\ddagger$ = 19.5 (2.6) kcal/mol; $\Delta H^\ddagger$ = 13.8 (1.0) kcal/mol; $\Delta S^\ddagger$ = −19.1 (4.3) eu. For a metal-to-nucleotide ratio of 0.5 (that used in the initial experiments—see Figures 1–3), τ_M^{-1} is estimated to be 2.02 (33) × 10^3 s^{-1} at 25 °C. Thus T_{1M}^{-1} can now be estimated from τ_M^{-1} and fT_{1p} with eq 1, yielding T_{1M}^{-1} = 150 (15) s^{-1} at 25 °C.

In order to obtain a reliable estimate of the V(IV)–^{31}P distance from eq 6, the correlation time, τ_c, should be estimated by more than one technique. The ^{31}P longitudinal paramagnetic relaxation rate was measured as a function of the applied magnetic field at ν = 36.19, 109.16, and 161.90 MHz. Assuming that τ_c is frequency-independent, the data can be fit by least-squares to the relationship:[47]

$$T_{1p} = \frac{1}{fC\tau_c}(1 + \omega_I^2\tau_c^2) \quad (8)$$

We thereby estimate τ_c = 0.74 (0.03) ns using this method. A final value for τ_c of 1.1 (0.4) ns is obtained by averaging this result with the estimate of τ_c obtained from the temperature dependence of T_{1p} (1.5 (5) ns, vide supra). This correlation time corresponds to a hydrodynamic radius for the metal–nucleotide complex of 10–14 Å.[48] Assuming that each V(IV) ion interacts with only one phosphate group at a time, the average V(IV)–^{31}P distance in the complex is estimated to be 6.2 (2) Å. If each V(IV) ion simultaneously interacts with two phosphate groups, then r = 5.5 (1) Å. These metal–^{31}P distances are in the range derived for "outer-sphere" (e.g., through a water bridge) complexation of a paramagnetic ion (e.g., Mn(II)) to a phosphate group.[22]

To test whether the dipolar term is indeed dominant in eq 2, an estimate of the electron–^{31}P nuclear superhyperfine coupling constant A is needed. Since τ_M decreases with increasing temperature, it is possible to estimate a lower limit for T_{2M}^{-1} from the high-temperature measurements.[22] A value of $T_{2M}^{-1} > 5.2 \times 10^3$ s^{-1} is obtained from T_{2p} measured at 70 °C (there was no evidence for the release of significant additional amounts of cyclopentadiene at this temperature). A lower limit for $A/\hbar$ can now be obtained from eq 3, taking $\tau_e = \tau_{1S} \approx 1.0$ ns. The equivalence of τ_e and τ_{1S} is reasonable since τ_M should be relatively large in eq 5.[22b] A lower limit for the superhyperfine term is thus estimated to be $A/\hbar \geq 3.14 \times 10^6$ Hz (or ≥1.1 G). An additional method of estimating the superhyperfine coupling term is by EPR.[49] EPR spectra were measured for aqueous Cp_2VCl_2 in the presence of the five nucleotides and phenyl phosphate at room temperature and at 77 °K. No ^{31}P superhyperfine coupling could be resolved, and it is estimated that the hyperfine coupling term cannot be greater than 2.5 G or 7.0 × 10^6 Hz. In contrast, ^{31}P superhyperfine coupling has been reported to be 8.5 G for a direct V–O–P linkage in a VO^{2+}–S-adenosylmethionine synthetase complex.[50] The estimated range for $A/\hbar$ of 3.1–7.0 × 10^6 Hz in the present case indicates a dipolar contribution of 40–70% to T_{1M}^{-1}. Due to the r^{-6} dependence of T_{1M}, neglecting the scalar contribution to T_{1M}^{-1} results in an error of only ca. 2% in r. Data of Granot et al.[22] show that for Mn(II)-induced relaxation of ^{31}P nuclei on a DNA fragment, T_{1M}^{-1} is composed of ≲78% dipolar and ≳22% scalar contributions.

That the interaction of aqueous Cp_2VCl_2 occurs predominantly at the phosphate groups of the nucleotides can now be confirmed by calculating the ^{1}H line broadening expected if Cp_2VCl_2 were interacting at the nitrogen sites of the purine or pyrimidine bases. With use of the previously estimated parameters of the correlation time (assuming that τ_c is the same for the ^{1}H as that for the ^{31}P nucleus), the lower limit for the superhyperfine coupling term, and τ_e, T_{2M}^{-1} can be calculated with eq 3 and thus yields a lower limit for the expected broadening. For a V^{IV}–N distance of r = 2 Å, the paramagnetic contribution to the resonance line width of a nearby proton is calculated to be >180 Hz. Since the greatest purine or pyrimidine proton line width measured in the presence of Cp_2VCl_2 is ca. 33 Hz, it can be seen that Cp_2VCl_2 interacts preferentially with the phosphate groups of the nucleotides.

Interaction of Cp_2VCl_2 with Alkylated Nucleobases. In order to further test whether the dominant mode of Cp_2VCl_2 interaction with the deoxyribonucleotide monophosphates is at the phosphate moiety, a series of experiments was carried out with alkylated nucleobases in the presence of the paramagnetic compound. Alkylation of the nucleobases at the site of the glycosidic linkage (N(1) or N(9)) would block a potential metal-binding site at the nitrogen atom in the purine or pyrimidine base (Chart I). These experiments were carried out in Me_2SO-d_6 solvent due to the limited solubility of the nucleobases in water. In the cases of 9-MeA, 9-EtG, and 1-MeT, no significant changes in any of the ^{1}H resonances were observed (broadening ≤2 Hz). In the case of 1-MeC, a slight selective broadening of the amino resonance relative to the other ^{1}H resonances is observed. The line width of the amino resonance is a linear function of the concentration of added Cp_2VCl_2. For an increasing metal-to-nucleotide ratio of 3.9 × 10^{-3} to 3.3 × 10^{-2}, the paramagnetic contribution to the line width increases from 19.4 to 30.3 Hz in a linear fashion. This result suggests that the V(IV) center binds preferentially in the proximity of the N(3) site of 1-MeC. The electrostatic potential energy map for 1-MeC reported by Kistenmacher et al.[51] shows that N(3) (pK_a = 4.4)[52] is by far the most favorable metal ion binding site available at pH 7. Additional ^{1}H NMR experiments indicate that the Watson–Crick hydrogen bonding present in mixtures of either 1-MeC and 9-EtG or 1-MeT and 9-MeA (1:1 molar ratio) is unaffected by the presence of Cp_2VCl_2 (up to 0.4 equiv).

Description of the Diaquabis(cyclopentadienyl)vanadium(IV) Diphenyl Phosphate (1) Crystal Structure. Complex **1** can be prepared by the reaction of eq 9. The X-ray structural analysis

$$Cp_2VCl_2 + 2HPO_2(OPh)_2 \xrightarrow[25\ °C]{H_2O} Cp_2V(OH_2)_2{\cdot}2O_2P(OPh)_2 + 2HCl(aq) \quad (9)$$

reveals that single crystals of **1** are composed of two crystallographically independent mononuclear $Cp_2V(OH_2)_2{\cdot}2O_2P(OPh)_2$ molecules. The H atoms of the water molecules (vide infra) could not be located. The V(IV) ion adopts the familiar "bent sandwich" geometry found in numerous Cp_2VX_n (n = 2[41,53–55] or 1[56–67])

(46) Reference 20d, p 178.
(47) Reference 20d, p 221.
(48) Chao, Y.-H. H.; Kearns, D. R. *J. Am. Chem. Soc.* **1977**, *99*, 6425–6434 and references therein.
(49) For a review of V(IV) EPR spectroscopy, see: Chasteen, N. D. In *Biological Magnetic Resonance*; Berliner, L. J., Reuben, J., Eds., Plenum Press: New York, 1981; Vol. 3, Chapter 2, pp 53–120.
(50) Markham, G. D. *Biochemistry*, **1984**, *23*, 470–478.
(51) Kistenmacher, T. J.; Orbell, J. D.; Marzilli, L. G., ref 11a, Chapter 9, pp 191–207.
(52) Reported for 0.1 M ionic strength near 25 °C; see: Martin, R. B. *Acc. Chem. Res.* **1985**, *18*, 32–38.
(53) Atwood, J. L.; Rogers, R. D.; Hunter, W. B.; Floriani, C.; Fachinetti, G.; Villa, A. C. *Inorg. Chem.* **1980**, *19*, 3812–3817.
(54) Muller, E. G.; Watkins, S. F.; Dahl, L. F. *J. Organomet. Chem.* **1976**, *111*, 73–89.
(55) Muller, E. G.; Petersen, J. L.; Dahl, L. F. *J. Organomet. Chem.* **1976**, *111*, 91–112.
(56) Evans, W. J.; Bloom, I.; Doedens, R. J. *J. Organomet. Chem.* **1984**, *265*, 249–255.
(57) Pasquali, M.; Leoni, P.; Floriani, C.; Chiesi-Villa, A.; Guastini, A. *Inorg. Chem.* **1983**, *22*, 841–844.
(58) Gambarotta, S.; Floriani, C.; Chiesi-Villa, A.; Guastini, C. *J. Am. Chem. Soc.* **1982**, *104*, 2019–2020.
(59) Pasquali, M.; Gambarotta, S.; Floriani, C.; Chiesi-Villa, A.; Guastini, C. *Inorg. Chem.* **1981**, *20*, 165–171.

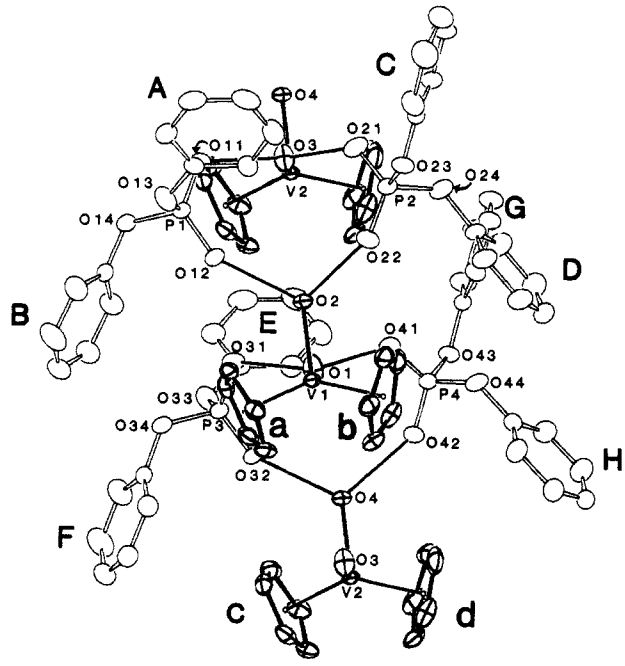

Figure 7. Perspective drawing of the molecular structure of $Cp_2V(OH_2)_2{\cdot}2O_2P(OPh)_2$ (**1**). In this and the following drawing the shapes of the ellipsoids correspond to 50% probability contours of atomic displacement, and the H atoms have been omitted. Lower-case letters denote cyclopentadienyl rings and upper-case letters phenyl rings. Numbering scheme for cyclopentadienyl rings: C6–C10(a), C1–C5(b), C16–C20(c), C11–C15(d). Numbering scheme for phenyl rings (numbered from C–O): C131–C136(A), C141–C146(B), C231–C236(C), C241–C246(D), C331–C336(E), C341–C346(F), C431–C436(G), C441–C446(H). A drawing with a more detailed numbering scheme is given in the supplemental material.

complexes, being π-bonded to two $C_5H_5^{-1}$ ligands and σ-bonded to two water molecules (vide infra). Final atomic coordinates and anisotropic displacement parameters for non-hydrogen atoms of crystalline **1** are presented in Tables II and III,[28] respectively. Bond lengths and angles involving non-hydrogen atoms of **1** are given in Tables IV and V, respectively. A perspective view of **1** is shown in Figure 7, and a stereoscopic view is shown in Figure 8.

Cp_2V^{2+} Coordination. The $C_5H_5^-$ ligation shows unexceptional intraligand metrical parameters. The average C–C distance (1.402 (3) Å), V–C distance (2.297 (5) Å), V–centroid distance (1.963 (2) Å), and ring centroid–V–ring centroid angle (133.0 (4)°) compare favorably with the corresponding metrical parameters in closely related molecules such as $(\eta^5\text{-}C_5H_4CH_3)_2VCl_2$ (C–C distance, 1.37 (1)–1.40 (1) Å; V–C distance, 2.37 (3) Å; V–centroid distance, 1.991 Å; ring centroid–V–ring centroid angle 133.4°),[41] as well as in other Cp_2V^{IV}-containing complexes.[53-55]

A crucial question regarding the V–O interaction is whether **1** is best described as containing $Cp_2V(OH_2)_2^{2+}$ ions (as in $Cp_2Ti(OH_2)_2^{2+}(NO_3^-)_2$[68] and $Cp_2Ti(OH_2)_2^{2+}(ClO_4^-)_2$[69]) or neutral

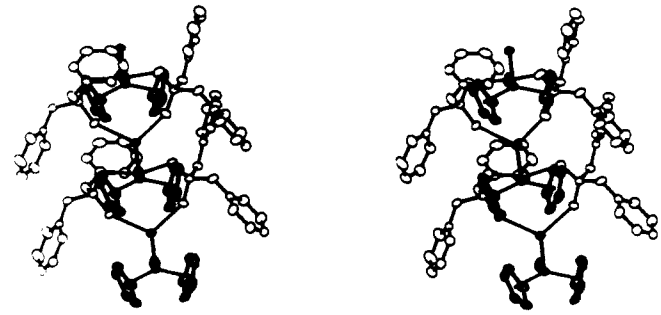

Figure 8. Stereoscopic view illustrating the infinite chains of molecules linked by hydrogen bonding in $Cp_2V(OH_2)_2{\cdot}2O_2P(OPh)_2$ (**1**). The *c* axis points from right to left, the *a* axis downwards, and the *b* axis out of the plane of the paper. Two adjacent vanadium complexes and the four phosphate molecules constitute the asymmetric unit; the parts of the two such chains that form the unit cell are well separated.

$Cp_2V(OH)_2$ units. The V–O distances in **1** range from 2.029 (3) to 2.067 (3) Å, with V–O(average) = 2.050 (3) Å. These parameters can be compared with V(IV)–OH_2 bond distances of 2.027 (12) Å in VO[pyridine-2,6-dicarboxylate]·$4H_2O$,[70] 2.02 (1) Å in VO[*N*-(2-pyridylmethyl)iminoacetate](H_2O)·$2H_2O$,[71] 2.281 (4) Å in VO[malonate]$_2(H_2O)^{2-}$,[72] 2.045 (3) Å in VO(F)(malonate)$(H_2O)_2^-$,[73] 2.018 (2) Å in VO{(*S*)-[[1-(2-pyridyl)ethyl]-imino]diacetate}(H_2O),[74] and 2.074 (3) Å in $V_2O_2F_6(H_2O)_2^{2-}$.[75] In contrast, V–OR single bond distances in comparable types of oxo–V(IV) complexes generally fall in the range 1.95–1.99 Å.[76,77] The data argue strongly for the $Cp_2V(OH_2)_2^{2+}$ formulation.

Diphenyl Phosphate Geometry. The metrical parameters for the diphenyl phosphate anion are typical of a diesterified phosphate anion.[78,79] The average P–OPh distance (e.g., P(1)–O(14)) of 1.601 (6) Å, P–O(non-ester) distance (e.g., P(1)–O(12)) of 1.480 (2) Å, and O–C(phenyl) distance of 1.392 (3) Å, as well as the O–P–O angles, compare favorably with the corresponding metrical parameters reported for the magnesium salts of the diethyl phosphate anion[78] and of the diphenyl phosphate anion $((PhO)_2PO_2)_6Mg_3(H_2O)_5$.[79] One exception is the occurrence of several rather small PhO–P–OPh angles in **1** (O(13)–P(1)–O(14), O(33)–P(3)–O(34) average = 99.6 (1)°), compared to the larger O(23)–P(2)–O(24), O(43)–P(4)–O(44) average of 104.0 (1)°. The corresponding angles reported for magnesium diethyl phosphate and magnesium diphenyl phosphate are 108.2 (4)°[78] and 104.0 (3)°,[79] respectively.

Hydrogen bonding. Each non-ester oxygen atom of the diphenyl phosphate anion participates in a hydrogen bond to vanadium-bound water molecules from two different $Cp_2V(OH_2)_2^{2+}$ cations, producing an infinite chain of hydrogen bonding throughout the crystal lattice (Figure 8). The average V–O–H···O–P oxygen-oxygen contact of 2.570 (5) Å is in the range of a strong hydrogen bond.[80]

(60) Facinetti, G.; Floriani, C.; Chiesi-Villa, A.; Gaustini, C. *J. Chem. Soc., Dalton Trans.* **1979**, 1612–1617.
(61) Gambarotto, S.; Pasquali, M.; Floriani, C.; Chiesi-Villa, A.; Guastini, C. *Inorg. Chem.* **1981**, *20*, 1173–1178.
(62) Pasquali, M.; Floriani, C.; Chiesi-Villa, A.; Guastini, C. *Inorg. Chem.* **1980**, *19*, 3847–3850.
(63) Köhler, F. H.; Prössdorf, W.; Schubert, U.; Neugebauer, D. *Angew. Chem., Int. Ed. Engl.* **1978**, *17*, 850–851.
(64) Smart, J. C.; Pinsky, B. L.; Fredrich, M. L.; Day, V. W. *J. Am. Chem. Soc.* **1979**, *101*, 4371–4373.
(65) Veith, M. *Angew. Chem., Int. Ed. Engl.* **1976**, *15*, 387–388.
(66) Fachinetti, G.; Del Nero, S.; Floriani, C. *J. Chem. Soc., Dalton Trans.* **1976**, 1046–1049.
(67) Fieselmann, B. F.; Stucky, G. D. *J. Organomet. Chem.* **1977**, *137*, 43–54.
(68) Klein, H.-P.; Thewalt, U. *Z. Anorg. Allg. Chem.* **1981**, *476*, 62–68.
(69) Thewalt, U.; Klein, H.-P. *J. Organomet. Chem.* **1980**, *194*, 297–307.
(70) Bersted, B. H.; Belford, R. L.; Paul, I. C. *Inorg. Chem.* **1968**, *7*, 1557–1562.
(71) Oci, S.; Nishizawa, M.; Matsumoto, K.; Kuroya, H.; Saito, K. *Bull. Chem. Soc. Jpn.* **1979**, *52*, 452–457.
(72) Pajunen, A.; Pajunen, S. *Acta Crystallogr., Sect B* **1980**, *36*, 2425–2428.
(73) Edwards, A. J.; Slim, D. R.; Sala-Pala, J.; Guerchais, J. E. *Bull. Soc. Chim. Fr.* **1975**, 2015–2018.
(74) Kojima, A.; Okazaki, K.; Ooi, S.; Saito, K. *Inorg. Chem.* **1983**, *22*, 1168–1174.
(75) Bukovec, P.; Milicev, S.; Demsar, A.; Golic, L. *J. Chem. Soc., Dalton Trans.* **1981**, 1802–1806.
(76) (a) Clark, R. J. H. In *Comprehensive Inorganic Chemistry*; Bailar, J. C., Emeleus, H. J., Nyholm, R. S., Trotman-Dickenson, A. F., Eds.; Pergamon: Oxford, 1980; Vol. 3, pp 514–516. (b) Chasteen, N. D.; Belford, R. L.; Paul, I. C. *Inorg. Chem.* **1969**, *8*, 408–418 and references therein.
(77) Wieghardt, K.; Bossek, U.; Volckmar, K.; Swiridoff, W.; Weiss, J. *Inorg. Chem.* **1984**, *23*, 1387–1389.
(78) Ezra, F. S.; Collin, R. L. *Acta Crystallogr.* **1973**, *B29*, 1398–1403.
(79) Narayanan, P.; Ramirez, F.; McCaffrey, T.; Chaw, Y.; Marecek, J. F. *J. Org. Chem.* **1978**, *43*, 24–31.

Table II. Positional Parameters and Equivalent B Values for the Atoms of $Cp_2V(OH_2)_2 \cdot 2O_2P(OPh)_2$ (**1**)[a]

atom	x	y	z	B_{eq} (Å^2)	atom	x	y	z	B_{eq} (Å^2)
V(1)	0.67935 (5)	0.5	0.27761 (2)	1.447 (9)	C(132)	0.1513 (3)	0.7143 (3)	0.3109 (1)	2.30 (7)
V(2)	0.16767 (5)	0.19011 (5)	0.26795 (2)	1.437 (9)	C(133)	0.0673 (4)	0.7835 (4)	0.2795 (2)	3.01 (8)
P(1)	0.26147 (8)	0.52065 (8)	0.38526 (3)	1.68 (1)	C(134)	−0.0147 (4)	0.8518 (3)	0.3022 (2)	3.09 (8)
P(2)	0.19968 (8)	0.56646 (9)	0.17088 (4)	2.30 (2)	C(135)	−0.0118 (4)	0.8517 (3)	0.3573 (2)	2.93 (8)
P(3)	0.75522 (8)	0.15007 (8)	0.37731 (3)	1.80 (1)	C(136)	0.0715 (4)	0.7834 (3)	0.3893 (2)	2.47 (7)
P(4)	0.68068 (8)	0.15107 (8)	0.15907 (3)	1.98 (2)	C(141)	0.4163 (3)	0.4717 (3)	0.4731 (1)	1.82 (6)
O(1)	0.6533 (3)	0.3337 (2)	0.2747 (1)	3.05 (6)	C(142)	0.4562 (4)	0.5601 (4)	0.5051 (2)	2.97 (8)
O(2)	0.4851 (2)	0.5059 (3)	0.27515 (9)	2.97 (5)	C(143)	0.5766 (4)	0.5572 (4)	0.5357 (2)	3.75 (9)
O(3)	0.1314 (3)	0.3576 (2)	0.2723 (1)	2.77 (5)	C(144)	0.6548 (4)	0.4661 (4)	0.5346 (2)	3.12 (8)
O(4)	−0.0271 (2)	0.1755 (3)	0.26484 (9)	2.71 (5)	C(145)	0.6132 (4)	0.3774 (4)	0.5025 (2)	3.06 (8)
O(11)	0.1404 (2)	0.4698 (2)	0.3592 (1)	2.04 (5)	C(146)	0.4934 (4)	0.3795 (3)	0.4712 (2)	2.75 (8)
O(12)	0.3764 (2)	0.5148 (3)	0.35859 (9)	2.89 (5)	C(231)	0.0232 (3)	0.7128 (3)	0.1304 (1)	1.90 (6)
O(13)	0.2331 (3)	0.6475 (2)	0.4001 (1)	2.62 (5)	C(232)	−0.0658 (3)	0.6363 (3)	0.1087 (1)	2.22 (7)
O(14)	0.2928 (2)	0.4706 (2)	0.44387 (9)	2.20 (5)	C(233)	−0.1882 (3)	0.6723 (4)	0.0885 (2)	3.00 (8)
O(21)	0.1039 (2)	0.5066 (3)	0.1970 (1)	3.25 (5)	C(234)	−0.2197 (4)	0.7818 (4)	0.0900 (2)	3.87 (9)
O(22)	0.3296 (3)	0.5885 (3)	0.1992 (1)	3.80 (7)	C(235)	−0.1289 (4)	0.8591 (4)	0.1121 (2)	3.9 (1)
O(23)	0.1475 (2)	0.6860 (2)	0.15162 (9)	2.23 (5)	C(236)	−0.0064 (4)	0.8244 (3)	0.1319 (2)	2.93 (8)
O(24)	0.2065 (2)	0.5009 (2)	0.1159 (1)	2.61 (5)	C(241)	0.3103 (3)	0.5056 (3)	0.0875 (1)	2.09 (6)
O(31)	0.6343 (2)	0.2072 (2)	0.3550 (1)	2.16 (5)	C(242)	0.3766 (4)	0.6014 (3)	0.0820 (2)	2.83 (8)
O(32)	0.8679 (2)	0.1589 (3)	0.34951 (9)	2.72 (5)	C(243)	0.4774 (4)	0.5982 (4)	0.0516 (2)	3.23 (8)
O(33)	0.7255 (3)	0.0222 (2)	0.3876 (1)	2.68 (5)	C(244)	0.5109 (4)	0.5018 (5)	0.0292 (2)	3.43 (9)
O(34)	0.7921 (2)	0.1906 (2)	0.43772 (9)	2.32 (5)	C(245)	0.4429 (4)	0.4055 (4)	0.0355 (2)	3.74 (9)
O(41)	0.5961 (2)	0.2064 (2)	0.1927 (1)	2.69 (5)	C(246)	0.3411 (4)	0.4076 (4)	0.0647 (2)	3.14 (8)
O(42)	0.8127 (2)	0.1176 (2)	0.1813 (1)	2.73 (5)	C(331)	0.6454 (3)	−0.0399 (3)	0.3506 (2)	2.17 (7)
O(43)	0.6135 (2)	0.0403 (2)	0.13300 (9)	2.03 (5)	C(332)	0.6450 (4)	−0.0302 (3)	0.2963 (2)	2.61 (7)
O(44)	0.6825 (2)	0.2322 (2)	0.1089 (1)	2.51 (5)	C(333)	0.5623 (4)	−0.0966 (4)	0.2621 (2)	3.19 (8)
C(1)	0.6219 (4)	0.5998 (3)	0.1998 (1)	2.61 (7)	C(334)	0.4800 (4)	−0.1708 (4)	0.2814 (2)	3.40 (9)
C(2)	0.6328 (4)	0.4876 (4)	0.1871 (1)	2.86 (8)	C(335)	0.4826 (4)	−0.1796 (4)	0.3364 (2)	3.26 (9)
C(3)	0.7639 (4)	0.4569 (4)	0.2015 (2)	3.08 (8)	C(336)	0.5654 (4)	−0.1134 (3)	0.3715 (2)	2.60 (7)
C(4)	0.8292 (3)	0.5501 (4)	0.2238 (2)	2.87 (8)	C(341)	0.9182 (2)	0.1862 (3)	0.4640 (1)	2.01 (6)
C(5)	0.7412 (4)	0.6378 (3)	0.2229 (1)	2.50 (7)	C(342)	0.9611 (4)	0.0913 (4)	0.4910 (2)	3.26 (9)
C(6)	0.6582 (3)	0.5747 (3)	0.3609 (1)	2.04 (6)	C(343)	1.0855 (5)	0.0899 (4)	0.5187 (2)	4.0 (1)
C(7)	0.7543 (3)	0.6336 (3)	0.3405 (1)	2.25 (7)	C(344)	1.1636 (4)	0.1822 (4)	0.5191 (2)	3.30 (8)
C(8)	0.8547 (3)	0.5594 (4)	0.3358 (2)	2.52 (7)	C(345)	1.1185 (4)	0.2758 (4)	0.4929 (2)	2.74 (8)
C(9)	0.8192 (3)	0.4545 (4)	0.3511 (1)	2.57 (7)	C(346)	0.9944 (4)	0.2780 (3)	0.4647 (1)	2.45 (7)
C(10)	0.6962 (3)	0.4629 (3)	0.3667 (1)	2.15 (7)	C(431)	0.4851 (3)	0.0310 (3)	0.1113 (1)	1.80 (6)
C(11)	0.1089 (4)	0.1108 (4)	0.1850 (2)	3.70 (9)	C(432)	0.4096 (3)	0.1202 (3)	0.0934 (1)	2.14 (7)
C(12)	0.1260 (4)	0.2254 (4)	0.1791 (1)	3.68 (9)	C(433)	0.2821 (3)	0.1024 (3)	0.0709 (2)	2.44 (7)
C(13)	0.2541 (4)	0.2490 (4)	0.1955 (2)	3.45 (9)	C(434)	0.2316 (3)	−0.0019 (4)	0.0665 (2)	2.73 (7)
C(14)	0.3166 (3)	0.1510 (4)	0.2120 (2)	2.97 (8)	C(435)	0.3089 (4)	−0.0903 (4)	0.0846 (2)	3.47 (9)
C(15)	0.2257 (4)	0.0663 (4)	0.2067 (2)	3.07 (8)	C(436)	0.4351 (4)	−0.0751 (3)	0.1077 (2)	2.73 (8)
C(16)	0.1517 (3)	0.1036 (3)	0.3486 (1)	2.33 (7)	C(441)	0.7806 (3)	0.2337 (3)	0.0774 (1)	2.16 (7)
C(17)	0.2469 (3)	0.0498 (3)	0.3256 (2)	2.39 (7)	C(442)	0.8520 (4)	0.3298 (3)	0.0779 (2)	2.76 (8)
C(18)	0.3465 (3)	0.1272 (4)	0.3231 (2)	2.68 (8)	C(443)	0.9488 (4)	0.3359 (4)	0.0461 (2)	3.12 (8)
C(19)	0.3095 (3)	0.2287 (3)	0.3429 (1)	2.34 (7)	C(444)	0.9720 (3)	0.2484 (4)	0.0146 (1)	2.77 (8)
C(20)	0.1868 (3)	0.2133 (3)	0.3580 (1)	2.09 (7)	C(445)	0.8995 (4)	0.1532 (4)	0.0143 (2)	3.31 (8)
C(131)	0.1519 (3)	0.7140 (3)	0.3659 (1)	1.87 (6)	C(446)	0.8032 (4)	0.1451 (4)	0.0459 (2)	2.81 (7)

[a] The equivalent displacement parameter is defined as $(4/3)\mathrm{Tr}(\beta \cdot G)$, where $\beta_{ij} = 2\pi^2 a^*_i a^*_j U_{ij}$.

The indirect binding of the vanadium atom to the phosphate group via a water bridge can be described by three different hydrogen-bonded linkages present in the crystal lattice. The first two modes are distinguished by the O(water)–O(non-ester)–P angle. The average vanadium–phosphorus distance in V(1)–P(1) and V(1)–P(2) is 5.48 (4) Å, with O(water)–O(non-ester)–P angles of 152.0 (1)° (O(2)–O(12)–P(1)) and 138.3 (2)° (O(2)–O(22)–P(2)), respectively (see Table V). The average vanadium–phosphorus distance in V(1)–P(3), V(1)–P(4), V(2)–P(1), and V(2)–P(2) is 5.07 (14) Å, with O(water)–O(non-ester)–P angles of 114.2 (2)° (O(1)–O(31)–P(3)), 129.8 (2)° (O(1)–O(41)–P(4)), 121.2 (2)° (O(3)–O(11)–P(1)), and 130.9 (1)° (O(3)–O(21)–P(2)), respectively. Finally, the average vanadium–phosphorus distance in V(2)–P(3), V(2)–P(4) and in V(1)–P(1), V(1)–P(2) (translating to the next unit cell along the a axis for V(1)) is 6.44 (7) Å.

(80) (a) Olovsson, I.; Jönsson, P.-G. In *The Hydrogen Bond*; Schuster, P., Zurdel, G., Sandarfy, C., Eds.; North-Holland: Amsterdam, 1976; Vol. 2, pp 393–456. (b) Bacon, G. E. *Neutron Scattering in Chemistry*; Butterworths: London, 1977; pp 39–68. (c) Joesten, M. D.; Schaad, L. J. *Hydrogen Bonding*; Marcel Dekker: New York, 1974; Chapter 6. (d) Novak, A. In *Structure and Bonding*; Dunitz, J. D., Hemmerich, P., Holm, R. H., Ibers, J. A., Jorgensen, C. K., Neilands, J. B., Reisen, D., Williams, R. J. P., Eds.; Springer-Verlag: New York, 1974; Vol. 18, pp 177–216. (e) Hamilton, W. C.; Ibers, J. A. *Hydrogen Bonding in Solids*; W. A. Benjamin: New York, 1968.

Discussion

This work provides the most complete picture to date of the mode of interaction of aqueous early transition metal Cp_2M^{2+} species with DNA components such as 2′-deoxyribonucleotide-5′-monophosphates, alkylated nucleobases, and phosphodiesters under conditions approximating physiological. Cp_2VCl_2 was chosen for the present studies both because of the hydrolytic stability of the Cp_2V^{2+} framework and because the electronic spin relaxation characteristics offer an NMR structural/dynamic probe of binding properties.

Interaction of Aqueous Cp_2VCl_2 with 2′-Deoxyribonucleotide-5′-monophosphates and Alkylated Nucleobases. The NMR relaxation studies indicate that near neutral pH, aqueous Cp_2VCl_2 binds selectively to the phosphate groups of nucleotides relative to the readily accessible nitrogenous sites on purine and pyrimidine bases. The interaction of aqueous Cp_2VCl_2 with the phosphate groups on nucleotides is a labile process, with the mean lifetime of the ligand–metal complex, τ_M = 0.49 (8) ms at 25 °C, as determined by ^{31}P relaxation time measurements on dAMP. That the dominant mode of interaction of Cp_2VCl_2 with the nucleotides occurs at the phosphate group is also indicated by the minor interaction of this complex with alkylated nucleobases, which have no phosphate moiety. The Watson–Crick hydrogen bonding (base-pairing) between nucleotides (e.g., dCMP and dGMP) in aqueous solution is not disrupted by the presence of Cp_2VCl_2, as

Table IV. Bond Lengths (Å) in $Cp_2V(OH_2)_2 \cdot 2O_2P(OPh)_2$ (**1**)[a]

atom 1	atom 2	distance	atom 1	atom 2	distance
V(1)	O(1)	2.029 (3)	V(2)	O(3)	2.067 (3)
V(1)	O(2)	2.047 (2)	V(2)	O(4)	2.058 (2)
V(1)	C(1)	2.308 (4)	V(2)	C(11)	2.304 (5)
V(1)	C(2)	2.270 (3)	V(2)	C(12)	2.263 (4)
V(1)	C(3)	2.296 (5)	V(2)	C(13)	2.277 (4)
V(1)	C(4)	2.316 (5)	V(2)	C(14)	2.314 (4)
V(1)	C(5)	2.319 (4)	V(2)	C(15)	2.300 (4)
V(1)	Cg1	1.968	V(2)	Cg3	1.961
V(1)	C(6)	2.330 (3)	V(2)	C(16)	2.317 (4)
V(1)	C(7)	2.320 (4)	V(2)	C(17)	2.309 (4)
V(1)	C(8)	2.302 (3)	V(2)	C(18)	2.304 (3)
V(1)	C(9)	2.260 (3)	V(2)	C(19)	2.280 (3)
V(1)	C(10)	2.274 (3)	V(2)	C(20)	2.268 (3)
V(1)	Cg2	1.961	V(2)	Cg4	1.961
C(1)	C(2)	1.403 (6)	C(11)	C(12)	1.408 (8)
C(2)	C(3)	1.428 (6)	C(12)	C(13)	1.387 (6)
C(3)	C(4)	1.395 (6)	C(13)	C(14)	1.390 (6)
C(4)	C(5)	1.409 (6)	C(14)	C(15)	1.397 (6)
C(5)	C(1)	1.386 (6)	C(15)	C(11)	1.383 (5)
C(6)	C(7)	1.400 (5)	C(16)	C(17)	1.396 (5)
C(7)	C(8)	1.408 (5)	C(17)	C(18)	1.418 (5)
C(8)	C(9)	1.393 (6)	C(18)	C(19)	1.402 (6)
C(9)	C(10)	1.417 (5)	C(19)	C(20)	1.418 (5)
C(10)	C(6)	1.412 (5)	C(20)	C(16)	1.387 (5)
O(1)	O(31)	2.572 (4)	O(3)	O(11)	2.569 (4)
O(1)	O(41)	2.576 (4)	O(3)	O(21)	2.602 (4)
O(2)	O(12)	2.547 (4)	O(4)	O(32)	2.558 (4)
O(2)	O(22)	2.538 (4)	O(4)	O(42)	2.597 (4)
P(1)	O(11)	1.483 (2)	P(3)	O(31)	1.488 (2)
P(1)	O(12)	1.476 (3)	P(3)	O(32)	1.474 (3)
P(1)	O(13)	1.618 (3)	P(3)	O(33)	1.606 (3)
P(1)	O(14)	1.587 (2)	P(3)	O(34)	1.595 (2)
P(2)	O(21)	1.478 (3)	P(4)	O(41)	1.482 (3)
P(2)	O(22)	1.475 (3)	P(4)	O(42)	1.482 (2)
P(2)	O(23)	1.597 (3)	P(4)	O(43)	1.611 (3)
P(2)	O(24)	1.609 (3)	P(4)	O(44)	1.605 (3)
O(13)	C(131)	1.381 (4)	O(33)	C(331)	1.386 (4)
O(14)	C(141)	1.401 (4)	O(34)	C(341)	1.399 (4)
O(23)	C(231)	1.382 (4)	O(43)	C(431)	1.391 (4)
O(24)	C(241)	1.399 (4)	O(44)	C(441)	1.396 (4)
C(131)	C(132)	1.387 (5)	C(331)	C(332)	1.375 (5)
C(132)	C(133)	1.380 (5)	C(332)	C(333)	1.389 (5)
C(133)	C(134)	1.382 (7)	C(333)	C(334)	1.388 (6)
C(134)	C(135)	1.386 (6)	C(334)	C(335)	1.389 (7)
C(135)	C(136)	1.377 (5)	C(335)	C(336)	1.400 (5)
C(136)	C(131)	1.38 (5)	C(336)	C(331)	1.384 (5)
C(141)	C(142)	1.368 (5)	C(341)	C(342)	1.375 (6)
C(142)	C(143)	1.387 (6)	C(342)	C(343)	1.394 (7)
C(143)	C(144)	1.379 (6)	C(343)	C(344)	1.388 (7)
C(144)	C(145)	1.376 (6)	C(344)	C(345)	1.360 (7)
C(145)	C(146)	1.389 (5)	C(345)	C(346)	1.397 (6)
C(146)	C(141)	1.387 (5)	C(346)	C(341)	1.370 (5)
C(231)	C(232)	1.375 (5)	C(431)	C(432)	1.376 (5)
C(232)	C(233)	1.389 (5)	C(432)	C(433)	1.400 (5)
C(233)	C(234)	1.367 (7)	C(433)	C(434)	1.367 (6)
C(234)	C(235)	1.395 (6)	C(434)	C(435)	1.382 (6)
C(235)	C(236)	1.382 (7)	C(435)	C(436)	1.387 (5)
C(236)	C(231)	1.387 (5)	C(436)	C(431)	1.385 (5)
C(241)	C(242)	1.371 (6)	C(441)	C(442)	1.384 (6)
C(242)	C(243)	1.403 (6)	C(442)	C(443)	1.393 (6)
C(243)	C(244)	1.366 (7)	C(443)	C(444)	1.369 (6)
C(244)	C(245)	1.389 (8)	C(444)	C(445)	1.382 (6)
C(245)	C(246)	1.392 (6)	C(445)	C(446)	1.388 (7)
C(246)	C(241)	1.378 (6)	C(446)	C(441)	1.378 (6)

[a] Numbers in parentheses are estimated standard deviations in the least significant digits. Cg1, Cg2, Cg3, and Cg4 are the centroids of the rings composed of atoms C(1) to C(5), C(6) to C(10), C(11) to C(15), and C(16) to C(20), respectively.

shown by ^{1}H NMR studies at −5 °C.

In marked contrast to the vanadocene dichloride results, the mode of interaction of cisplatin with nucleotides involves a kinetically nonlabile, covalent bond to the endocyclic nitrogen atoms of the purine or pyrimidine bases (preferentially to N-7 of guanosine or N-3 of cytidine).[11,12] Cisplatin has also been shown to significantly affect the Watson–Crick hydrogen bonding between guanosine and cytidine.[38] Binding of platinum at N(7) of guanosine decreases the pK_a of N(1) from about 9.4 to 8.0,[81] thus facilitating deprotonation of N(1) at physiological pH. It is thus possible to form three hydrogen bonds between N(7)–platinated guanine and the N(7)–platinated guanine monanion, which may ultimately induce mutagenesis.[81] Interestingly, cisplatin has been shown to induce mutagenesis,[82] while Cp_2TiCl_2 apparently does not.[83]

A detailed study of the effect of Cp_2VCl_2 on the longitudinal (T_1) and transverse (T_2) ^{31}P relaxation times of dAMP allows an estimation of the average distance (r) in the solution complex between the paramagnetic probe and the phosphorus nucleus. The analysis is simplified by assuming that the spin–lattice relaxation mechanism is predominantly dipolar in nature. That this assumption is valid is suggested by the temperature dependence of T_{2p} (indicative of slow chemical exchange), as well as by an estimate of the magnitude of the electron–^{31}P superhyperfine coupling constant. It is found that T_{1M}^{-1} is comprised of ca. 40–70% dipolar and ca. 30–60% scalar contributions. Neglecting the significant scalar contribution to T_{1M}^{-1} results in only ca. 2% error in the calculated value for r. An estimate of the dipolar correlation time, τ_c, is necessary to calculate r (eq 6). By using two independent methods, τ_c is estimated to be 1.1 (0.4) ns. This value agrees favorably with the τ_c of adenosine in the presence of Cu(II) or Mn(II) (τ_c = 0.4 ns),[84-86] as well as with that estimated for free 5′-AMP (1.0 ns).[87] Assuming each V(IV) ion interacts with only one phosphate group at a time, r is estimated to be 6.2 (2) Å. If each V(IV) ion simultaneously interacts with two phosphate groups, r is estimated to be 5.5 (1) Å.

The aforementioned results take on particular significance when considered in light of the crystal structure of $Cp_2V(OH_2)_2 \cdot 2O_2P(OPh)_2$ (**1**), in which the vanadium–phosphorus nonbonded contacts are in the range of 5.07–6.44 Å. The agreement between the average vanadium–phosphorus internuclear distance estimated by the solution spectroscopic studies of the nucleotides in the presence of Cp_2VCl_2 and that of the X-ray crystallographic study of **1** lends credence to the notion that Cp_2V^{2+} can preferentially interact with nucleotide phosphate groups via a water bridge. NMR evidence for outer-sphere metal–phosphate complexation has previously been provided for 5′-GMP in the presence of Mn(II),[88] and for a DNA fragment in the presence of Mn(II) or Co(II),[22] as well as for numerous Mn(II) enzyme–substrate complexes.[89]

Qualitatively, the preference of Cp_2V^{2+} for bases such as water vis-à-vis that of $(NH_3)_2Pt^{2+}$ for nitrogenous sites of purine and pyrimidine bases can be rationalized on the basis of simple "hard" and "soft" considerations.[90] Ions such as Cp_2V^{2+} are relatively "hard" acids while $(NH_3)_2Pt^{2+}$ is relatively "soft". Interestingly, recent crystallographic studies of chlorobis(η^5-cyclopentadienyl)(purinato)titanium(IV)[91] indicate that Ti^{IV}–N(nucleotide) interactions are, in principle, possible. However, this

(81) Hitchcock, A. P.; Lock, C. J. L.; Pratt, W. M. C.; Lippert, B., ref 11a, pp 209–227.
(82) Lecointe, R.; Macquet, J.-P.; Butour, J.-L.; Paoletti, C. *Mutat. Res.* **1977**, *48*, 139–144.
(83) Simmon, V. F. *J. Natl. Cancer. Inst.* **1979**, *62*, 893–899.
(84) (a) Shulman, R. G.; Sternlicht, H.; Wyluda, J. *J. Chem. Phys.* **1965**, *43*, 3116–3122. (b) Sternlicht, H.; Shulman, R. G.; Anderson, E. W. *J. Chem. Phys.* **1965**, *43*, 3123–3132.
(85) Levy, G. C.; Dechter, J. J. *J. Am. Chem. Soc.* **1980**, *102*, 6191–6196.
(86) Missen, A. W.; Natusch, D. F. S.; Porter, L. J. *Aust. J. Chem.* **1972**, *25*, 129–135.
(87) Imoto, T.; Akasaka, K.; Hatano, H. *Chem. Phys. Lett.* **1975**, *32*, 86–89.
(88) Tajmir-Riahi, H. A.; Theophanides, T. *Can. J. Chem.* **1983**, *61*, 1813–1822.
(89) Mildvan, A. S. *Acc. Chem. Res.* **1977**, *10*, 246–252.
(90) (a) Pearson, R. G., Ed. *Hard and Soft Acids and Bases*; Dowden, Hutchinson, and Ross: Stroudsburg, PA, 1973. (b) Marzilli, L. G. In *Metal Ions in Genetic Information Transfer*; Eichhorn, G. L., Marzilli, L. G., Eds.; Elsevier/North-Holland: New York, 1981; Chapter 2.
(91) Beauchamp, A. L.; Cozak, D.; Mardhy, A. *Inorg. Chim. Acta* **1984**, *92*, 191–197.

Table V. Selected Bond Angles (deg) in $Cp_2V(OH_2)_2 \cdot 2O_2P(OPh)_2$ (**1**)[a]

atom 1	atom 2	atom 3	angle	atom 1	atom 2	atom 3	angle
O(1)	V(1)	O(2)	84.4 (1)	O(3)	V(2)	O(4)	83.9 (1)
O(1)	V(1)	Cg1	107.1	O(3)	V(2)	Cg3	107.1
O(1)	V(1)	Cg2	107.2	O(3)	V(2)	Cg4	106.6
O(2)	V(1)	Cg1	107.7	O(4)	V(2)	Cg3	107.1
O(2)	V(1)	Cg2	107.2	O(4)	V(2)	Cg4	107.9
Cg1	V(1)	Cg2	132.6	Cg3	V(2)	Cg4	133.3
C(2)	C(1)	C(5)	108.4 (3)	C(12)	C(11)	C(15)	107.7 (4)
C(1)	C(2)	C(3)	107.6 (3)	C(11)	C(12)	C(13)	107.8 (4)
C(2)	C(3)	C(4)	107.3 (4)	C(12)	C(13)	C(14)	108.3 (5)
C(3)	C(4)	C(5)	108.3 (3)	C(13)	C(14)	C(15)	107.9 (3)
C(1)	C(5)	C(4)	108.4 (4)	C(11)	C(15)	C(14)	108.3 (4)
C(7)	C(6)	C(10)	108.3 (3)	C(17)	C(16)	C(20)	109.0 (3)
C(6)	C(7)	C(8)	107.8 (3)	C(16)	C(17)	C(18)	107.4 (3)
C(7)	C(8)	C(9)	108.6 (3)	C(17)	C(18)	C(19)	108.2 (3)
C(8)	C(9)	C(10)	108.0 (3)	C(18)	C(19)	C(20)	107.2 (3)
C(6)	C(10)	C(9)	107.4 (3)	C(16)	C(20)	C(19)	108.2 (3)
O(31)	O(1)	O(41)	104.0 (1)	O(11)	O(3)	O(21)	104.1 (1)
O(12)	O(2)	O(22)	106.7 (1)	O(32)	O(4)	O(42)	110.2 (1)
V(1)	O(1)	O(31)	125.9 (1)	V(2)	O(3)	O(11)	125.4 (1)
V(1)	O(1)	O(41)	129.4 (1)	V(2)	O(3)	O(21)	129.8 (1)
V(1)	O(2)	O(12)	123.4 (1)	V(2)	O(4)	O(32)	122.1 (1)
V(1)	O(2)	O(22)	124.8 (1)	V(2)	O(4)	O(42)	125.6 (1)
O(1)	O(31)	P(3)	114.2 (2)	O(3)	O(11)	P(1)	121.2 (2)
O(1)	O(41)	P(4)	129.8 (2)	O(3)	O(21)	P(2)	130.9 (2)
O(2)	O(12)	P(1)	152.0 (1)	O(4)	O(32)	P(3)	152.3 (1)
O(2)	O(22)	P(2)	138.3 (2)	O(4)	O(42)	P(4)	134.2 (2)
O(11)	P(1)	O(12)	119.5 (1)	O(31)	P(3)	O(32)	119.8 (1)
O(11)	P(1)	O(13)	108.5 (1)	O(31)	P(3)	O(33)	109.3 (1)
O(11)	P(1)	O(14)	107.6 (1)	O(31)	P(3)	O(34)	107.0 (1)
O(12)	P(1)	O(13)	110.1 (2)	O(32)	P(3)	O(33)	109.8 (2)
O(12)	P(1)	O(14)	109.6 (1)	O(32)	P(3)	O(34)	109.5 (1)
O(13)	P(1)	O(14)	99.6 (1)	O(33)	P(3)	O(34)	99.6 (1)
O(21)	P(2)	O(22)	121.5 (2)	O(41)	P(4)	O(42)	121.4 (1)
O(21)	P(2)	O(23)	110.6 (2)	O(41)	P(4)	O(43)	110.1 (1)
O(21)	P(2)	O(24)	105.4 (2)	O(41)	P(4)	O(44)	104.8 (1)
O(22)	P(2)	O(23)	103.9 (2)	O(42)	P(4)	O(43)	105.1 (1)
O(22)	P(2)	O(24)	110.4 (2)	O(42)	P(4)	O(44)	110.2 (1)
O(23)	P(2)	O(24)	103.9 (1)	O(43)	P(4)	O(44)	104.1 (1)
P(1)	O(13)	C(131)	121.9 (2)	P(3)	O(33)	C(331)	121.8 (2)
P(1)	O(14)	C(141)	122.4 (2)	P(3)	O(34)	C(341)	121.6 (2)
P(2)	O(23)	C(231)	126.6 (2)	P(4)	O(43)	C(431)	125.1 (2)
P(2)	O(24)	C(241)	124.2 (2)	P(4)	O(44)	C(441)	123.7 (2)
O(13)	C(131)	C(132)	122.4 (4)	O(33)	C(331)	C(332)	122.5 (3)
O(13)	C(131)	C(136)	116.7 (3)	O(33)	C(331)	C(336)	116.0 (3)
C(132)	C(131)	C(136)	120.9 (4)	C(332)	C(331)	C(336)	121.6 (3)
C(131)	C(132)	C(133)	118.8 (3)	C(331)	C(332)	C(333)	118.6 (4)
C(132)	C(133)	C(134)	121.0 (4)	C(332)	C(333)	C(334)	121.6 (4)
C(133)	C(134)	C(135)	119.6 (4)	C(333)	C(334)	C(335)	118.8 (4)
C(134)	C(135)	C(136)	120.5 (4)	C(334)	C(335)	C(336)	120.4 (4)
C(131)	C(136)	C(135)	119.5 (4)	C(331)	C(336)	C(335)	119.1 (4)
O(14)	C(141)	C(142)	120.0 (3)	O(34)	C(341)	C(342)	119.2 (3)
O(14)	C(141)	C(146)	118.7 (3)	O(34)	C(341)	C(346)	119.5 (3)
C(142)	C(141)	C(146)	121.3 (3)	C(342)	C(341)	C(346)	121.3 (3)
C(141)	C(142)	C(143)	119.0 (4)	C(341)	C(342)	C(343)	118.4 (4)
C(142)	C(143)	C(144)	120.9 (4)	C(342)	C(343)	C(344)	120.7 (5)
C(143)	C(144)	C(145)	119.5 (4)	C(343)	C(344)	C(345)	119.9 (4)
C(144)	C(145)	C(146)	120.4 (4)	C(344)	C(345)	C(346)	119.9 (4)
C(141)	C(146)	C(145)	119.0 (4)	C(341)	C(346)	C(345)	119.8 (3)
O(23)	C(231)	C(232)	123.6 (3)	O(43)	C(431)	C(432)	123.4 (4)
O(23)	C(231)	C(236)	115.0 (3)	O(43)	C(431)	C(436)	116.2 (3)
C(232)	C(231)	C(236)	121.5 (3)	C(432)	C(431)	C(436)	120.5 (4)
C(231)	C(232)	C(233)	118.7 (4)	C(431)	C(432)	C(433)	119.2 (3)
C(232)	C(233)	C(234)	120.8 (4)	C(432)	C(433)	C(434)	121.1 (3)
C(233)	C(234)	C(235)	120.2 (4)	C(433)	C(434)	C(435)	118.8 (3)
C(234)	C(235)	C(236)	119.6 (4)	C(434)	C(435)	C(436)	121.4 (4)
C(231)	C(236)	C(235)	119.3 (4)	C(431)	C(436)	C(435)	118.9 (3)
O(24)	C(241)	C(242)	122.5 (3)	O(44)	C(441)	C(442)	117.3 (3)
O(24)	C(241)	C(246)	115.6 (3)	O(44)	C(441)	C(446)	121.8 (3)
C(242)	C(241)	C(246)	121.9 (4)	C(442)	C(441)	C(446)	121.1 (4)
C(241)	C(242)	C(243)	118.2 (4)	C(441)	C(442)	C(443)	119.1 (4)
C(242)	C(243)	C(244)	121.0 (5)	C(442)	C(443)	C(444)	120.3 (4)
C(243)	C(244)	C(245)	119.8 (4)	C(443)	C(444)	C(445)	120.0 (4)
C(244)	C(245)	C(246)	120.0 (4)	C(444)	C(445)	C(446)	120.7 (5)
C(241)	C(246)	C(245)	119.1 (4)	C(441)	C(446)	C(445)	118.9 (4)

[a] Numbers in parentheses are estimated standard deviations in the least significant digits. Cg1, Cg2, Cg3, and Cg4 are the centroids of the rings composed of atoms C(1) to C(5), C(6) to C(10), C(11) to C(15), and C(16) to C(20), respectively.

complex was prepared in THF solution and appears to be hydrolytically unstable.

X-ray Crystallographic Study of $Cp_2V(OH_2)_2 \cdot 2O_2P(OPh)_2$ (1). The crystal structure of the product of the reaction between aqueous vanadocene dichloride and diphenyl phosphate (eq 9) shows that the interaction of vanadium(IV) with phosphate is an outer-sphere process. The structure is stabilized by a network of strong hydrogen bonds between $V-OH_2$ and $PO_2(OPh)_2^-$. That Cp_2V^{2+} prefers to bind to water and not diphenyl phosphate is, as already noted, consistent with such qualitative correlations as HSAB theory, in that OH_2 is a better "hard base" than diphenyl phosphate.[90]

Crystallographically characterized examples of outer-sphere metal–nucleotide phosphate complexation include the following: $[Ni(5'\text{-IMP})(H_2O)_5]$[92] (also containing a Ni–N(7) bond), $[Ni(5'\text{-AMP})(H_2O)_5]$[93] (also containing a Ni–N(7) bond), $(Co\text{-}5'\text{-IMP})(7H_2O)$ (also containing a Co–N(7) bond),[94] $[Cu(5'\text{-GMP})_3(8H_2O)\cdot 4H_2O)]_n$[95] (inner- and outer-sphere phosphate complexation), $Na_2[Cu(5'\text{-IMP})_2(dien)]\cdot 10H_2O$[96] (also containing a Cu–N(7) bond) (dien = diethylenetriamine), and most recently, $[Cu(bim)(H_2O)_5]^{2+}[5'\text{-IMP}]^{2-}\cdot 3H_2O$[97] (phosphate-only interaction; bim = benzimidazole).

The structure of **1** offers a tentative model for the interaction of Cp_2V^{2+} with DNA in that diesterified phosphoric acids exhibit metrical parameters about the phosphate similar to those in DNA.[98-100] Also, the average P–P separation in **1** of 7.04 (14) Å is similar to that found in oligonucleotides (e.g., 6.17–7.12 Å for the B DNA dodecamer d(CGCGAATTCGCG)).[98,99]

Conclusions

This study presents a solution spectroscopic analysis of the mode of interaction of the new antitumor agent Cp_2VCl_2 with nucleotides and model compounds thereof. Aqueous Cp_2VCl_2 has been shown to interact preferentially with the phosphate groups of nucleotides. ^{31}P nuclear relaxation time measurements show that aqueous Cp_2VCl_2 binds to the phosphate group of dAMP through a labile outer-sphere complexation. The average distance in solution between the paramagnetic center V(IV) and the ^{31}P nucleus is estimated to be 6.2 (2) or 5.5 (1) Å, if each V(IV) ion interacts with one or two phosphate groups, respectively. The crystal structure of $Cp_2V(OH_2)_2 \cdot 2O_2P(OPh)_2$ shows that vanadium binds to the phosphate groups via a water bridge, with vanadium–phosphorus nonbonded contacts ranging from 5.07 to 6.44 Å.

The present results indicate that Cp_2MCl_2 interactions with DNA are likely to be very different in character than those of cisplatin. While mechanistic speculation about the Cp_2MCl_2 systems would be premature at this stage, it is noteworthy that nonlabile, nitrogen-centered σ-bonding nucleobase interactions are by no means universal for drug–DNA complexes.[100] Indeed, systems which interact primarily by intercalative or electrostatic forces[100,101] and which can be relatively labile[100b,102] in binding can effect biologically significant changes in local DNA conformation, transcription, chromatin folding, etc. An interesting consequence of the present lability is that facile clearance of the drug might be expected. The lability of Cp_2V^{2+}–biomacromolecule interactions is supported by our recent observation[103] that vanadium from intraperitoneal Cp_2VCl_2 administration is cleared more rapidly from various organs of mice than is cisplatin. Further studies of Cp_2MCl_2/nucleotide, polynucleotide coordination chemistry are in progress.

Acknowledgment. This research was supported by the National Science Foundation under Grant CHE8306255.

Registry No. 1, 104051-71-0; Cp_2VCl_2, 12083-48-6; dAMP, 653-63-4; dCMP, 1032-65-1; dGMP, 902-04-5; dTMP, 365-07-1; dUMP, 964-26-1; 9-MeA, 700-00-5; 9-EtG, 879-08-3; 1-MeT, 4160-72-9; 1-MeC, 1122-47-0; diphenyl phosphate, 838-85-7.

Supplementary Material Available: Table of anisotropic displacement parameters (Table III) and a more detailed structural diagram of **1** (4 pages); a listing of observed and calculated structure factors from the final cycle of least-squares refinement for $Cp_2V(OH_2)_2 \cdot 2O_2P(OPh)_2$ (71 pages). Ordering information is given on any current masthead page.

(92) Clark, G. R.; Orbell, J. D. *J. Chem. Soc., Chem. Commun.* **1974**, 139–140.
(93) DeMeester, P.; Goodgame, D. M. L.; Skapski, A. C. *Biochim. Biophys. Acta* **1974**, *353*, 392–394.
(94) Aoki, K. *Bull. Chem. Soc. Jpn.* **1975**, *48*, 1260–1271.
(95) Aoki, K.; Clark, G. R.; Orbell, J. D. *Biochim. Biophys. Acta* **1976**, *425*, 369–371.
(96) Chiang, C. C.; Sorrell, T.; Kistenmacher, T. J.; Marzilli, L. G. *J. Am. Chem. Soc.* **1973**, *100*, 5102–5110.
(97) Poojary, D. M.; Begum, N. S.; Manshar, H.; Bau, R. *J. Chem. Soc., Chem. Commun.* **1985**, 821–822.
(98) Dunitz, J. D. Rollett, J. S. *Acta Crystallogr.* **1956**, *9*, 327–334.
(99) (a) Zimmermann, S. B.; Pheiffer, B. H. *J. Mol. Biol.* **1979**, *135*, 1023–1027. (b) Dickerson, R. E.; Drew, H. R. *J. Mol. Biol.* **1981**, *149*, 761–786.
(100) (a) Reference 39, Chapters 16 and 18. (b) Wilson, W. D.; Jones, R. L. In *Intercalation Chemistry*; Whittingham, M. S., Jacobson, A. J., Eds.; Academic: New York, 1982; Chapter 14. (c) Berman, H. M.; Young, P. R. *Annu. Rev. Biophys. Bioenerg.* **1981**, *10*, 87–114.
(101) Sen, D.; Crothers, D. M. *Biochemistry* **1986**, *25*, 1495–1503, 1503–1509, and references therein.
(102) Reference 20b, pp 525–527.
(103) Toney, J. H.; Murthy, M. S.; Marks, T. J. *Chem.-Biol. Interact.* **1985**, *56*, 45–54.